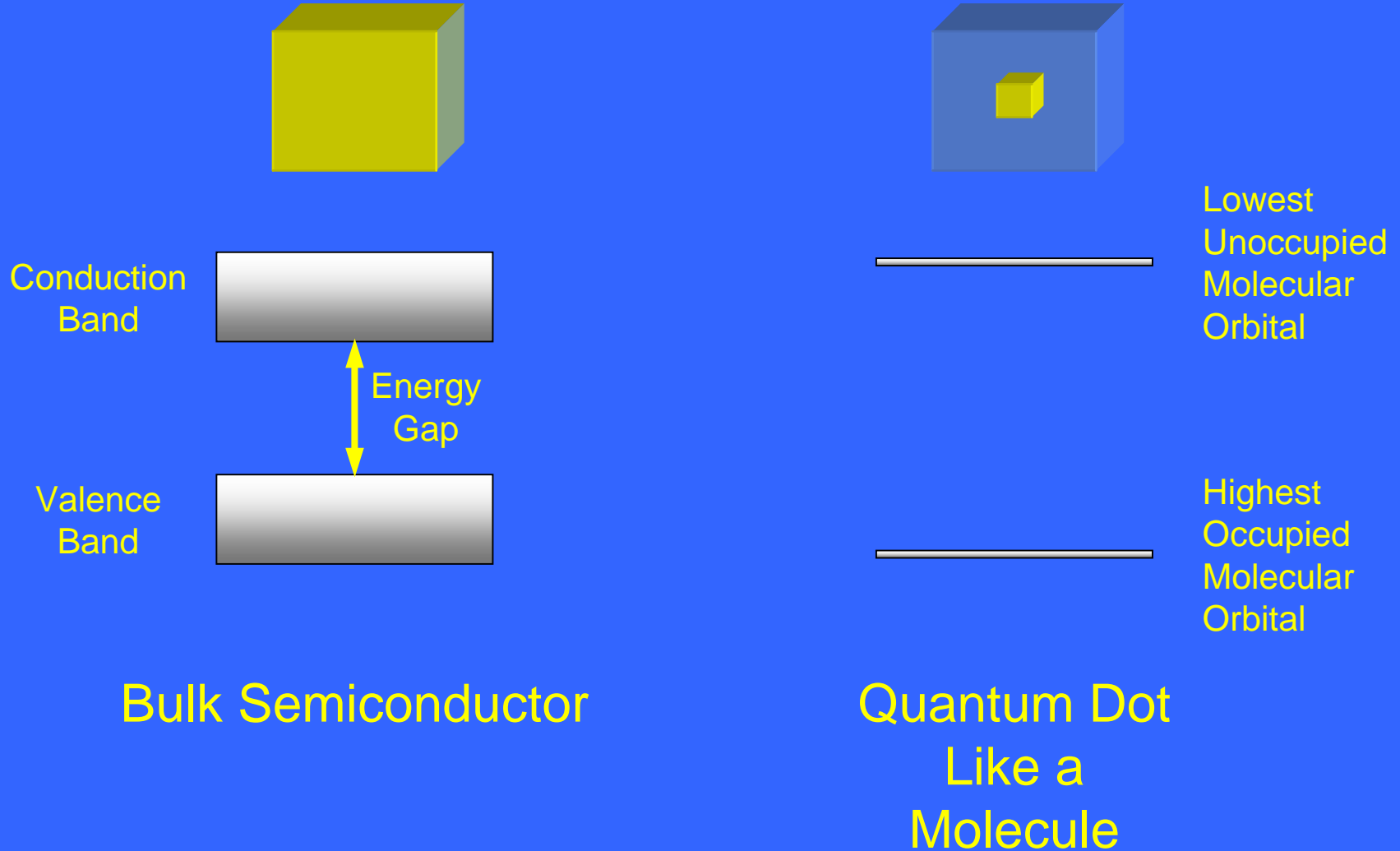


2004 Debye Lecture 3
C. B. Murray

Semiconductor Nanocrystals
Quantum Dots Part 1

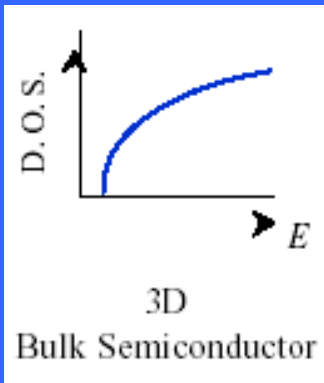
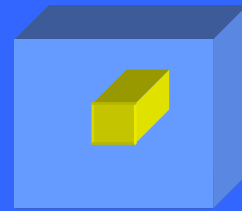
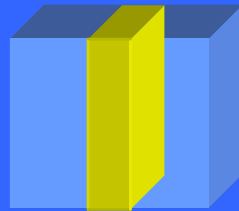
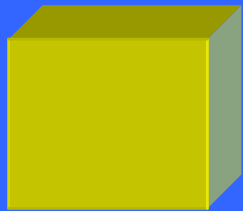
Basic Physics of Semiconductor Quantum Dots

C. R. Kagan, IBM T. J. Watson Research Center,
Yorktown Heights, NY

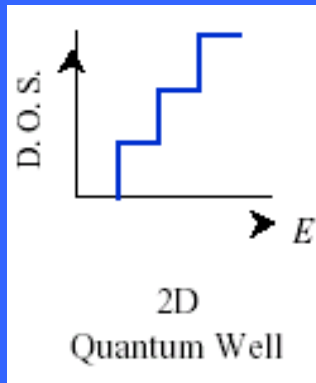


Quantum Confinement

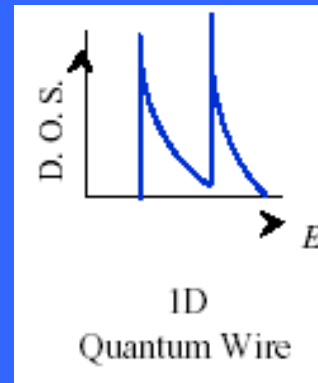
Low Dimensional Structures



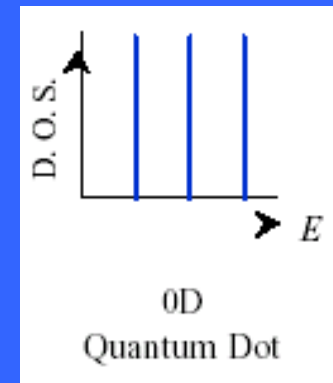
3D
Bulk Semiconductor



2D
Quantum Well



1D
Quantum Wire



0D
Quantum Dot

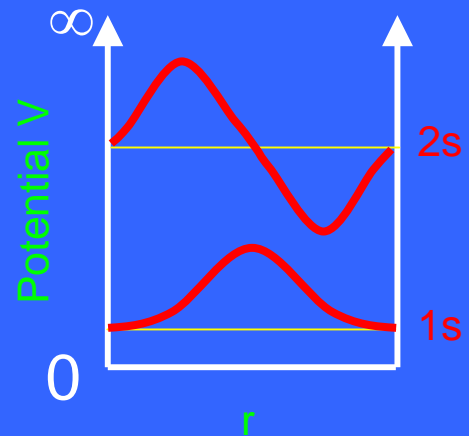
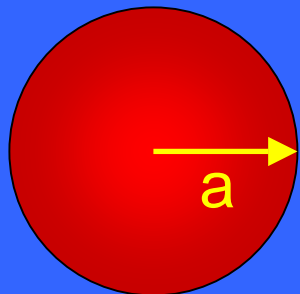
$$\rho_c(E) \propto \sqrt{(E - E_c)}$$

$$\rho_c(E) = \text{constant}$$

$$\rho_c(E) \propto \frac{1}{\sqrt{(E - E_n)}}$$

$$\rho_c(E) \propto \delta(E - E_n)$$

Particle-in-a-Sphere



solutions give
hydrogen-like orbitals with
quantum numbers
 n (1, 2, 3 ...)
 l (s, p, d ...)
 m

$$\Phi(r, \theta, \phi) = C \frac{j_l(k_{n,l}r)Y_l^m(\theta, \phi)}{r}$$

$Y_l^m(\theta, \phi)$ is a spherical harmonic

$j_l(k_{n,l}r)$ is the l^{th} order spherical Bessel function

$$k_{n,l} = \frac{\alpha_{n,l}}{a}$$



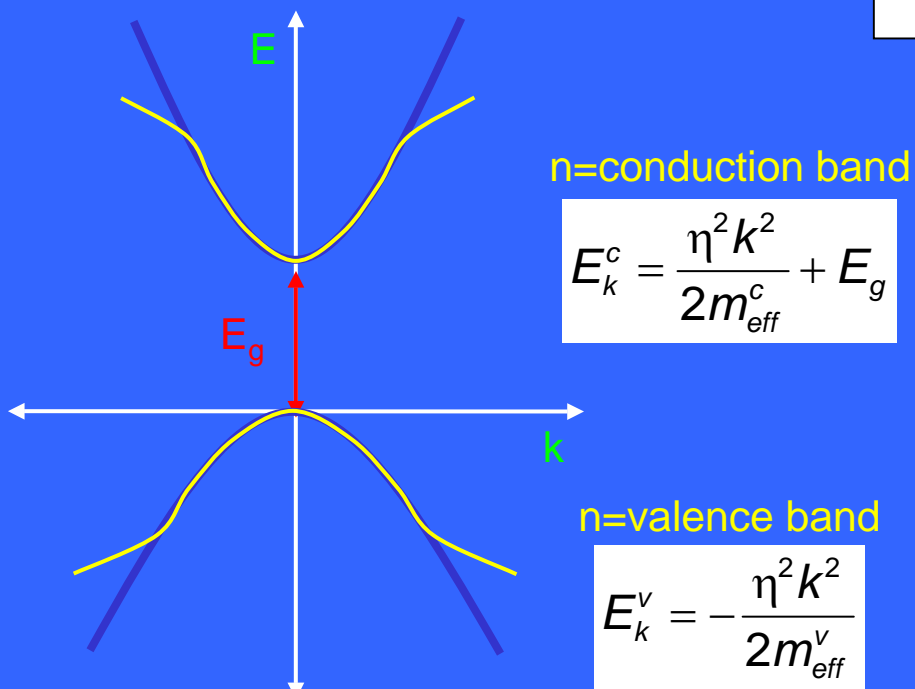
$$E_{n,l} = \frac{\eta^2 k_{n,l}^2}{2m_o} = \frac{\eta^2 \alpha_{n,l}^2}{2m_o a^2}$$

Discrete energy levels

size-dependence

The Quantum Dot is a Semiconductor

The Effective Mass Approximation
parabolic conduction and valence bands



Direct Bandgap Semiconductor

Bloch's Theorem

$$\Psi_{nk}(\vec{r}) = u_{nk}(\vec{r}) \exp(i\vec{k} \cdot \vec{r})$$

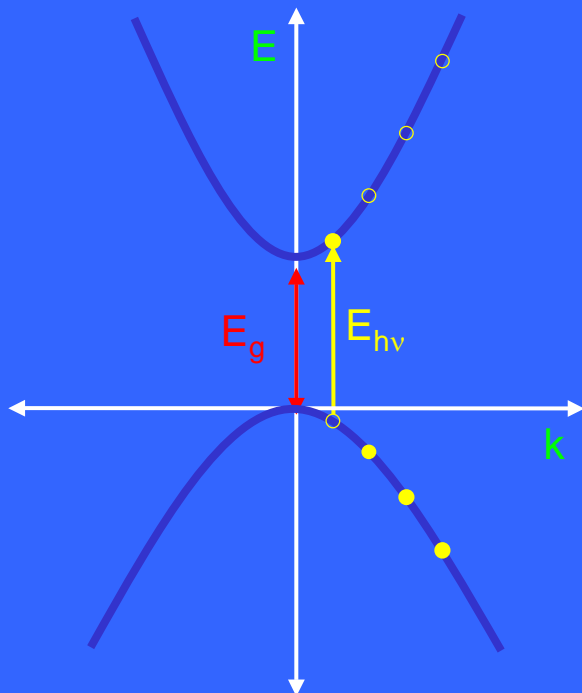
with periodicity of crystal lattice

Free particles treated by effective mass:

- describing graphically the curvature of the bands
- representing the potential presented by the lattice

Combining the Effective Mass Approximation with a Spherical Boundary Condition

Single Particle (sp) Wavefunction



$$(1) \quad \Psi_{sp}(\vec{r}) = \sum_k C_{nk} u_{nk}(\vec{r}) \exp(i\vec{k} \cdot \vec{r})$$

linear combination of Bloch functions

$$(2) \quad \Psi_{sp}(\vec{r}) = u_{n0}(\vec{r}) \sum_k C_{nk} \exp(i\vec{k} \cdot \vec{r}) = u_{n0}(\vec{r}) f_{sp}(\vec{r})$$

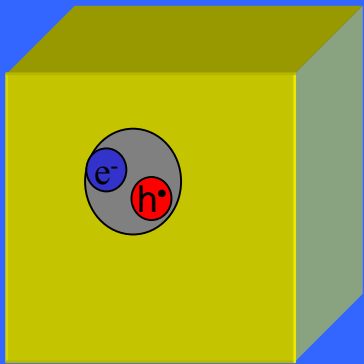
assume u_{nk} has weak k -dependence

Envelope Function Approximation
valid for $r_{QD} >$ lattice constant
which for QDs is given by
the “Particle-in-a-Sphere”

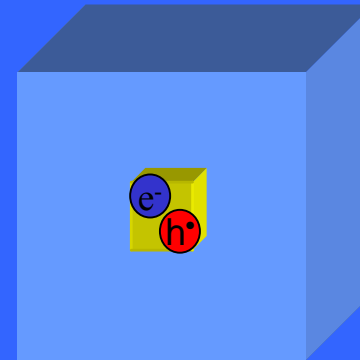
$$(3) \quad u_{n0}(\vec{r}) = \sum_i C_{ni} \varphi_n(\vec{r} - \vec{r}_i)$$

linear combination of atomic orbitals with
atomic wavefunctions φ_n (n = CB or VB)
 i =lattice sites

Coulomb Attraction



Bulk semiconductors,
Coulomb attraction
creates bound excitons



Confinement Energy $\propto 1/a^2$
Coulomb Attraction $\propto 1/a$

For small a :

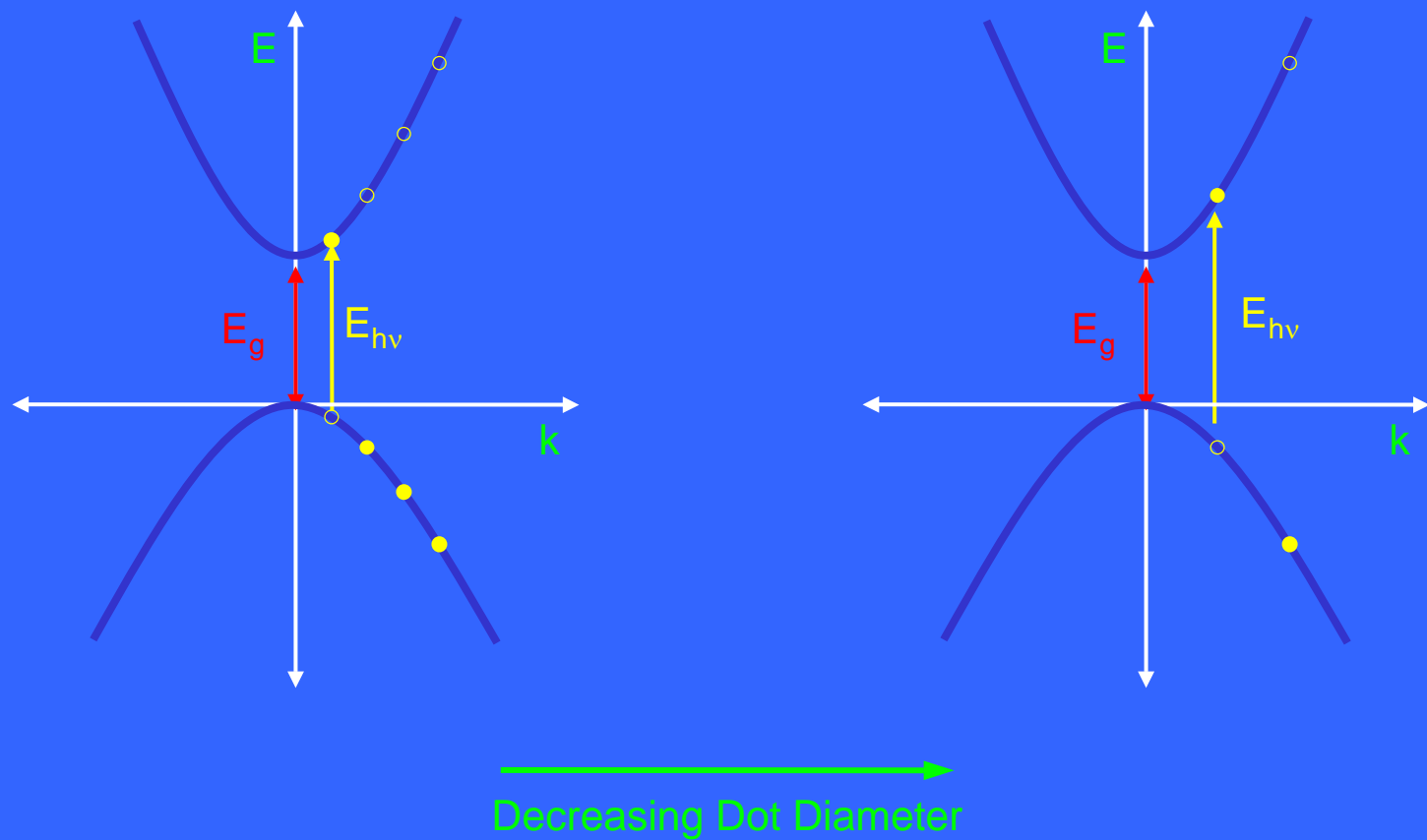
- Confinement Energy > Coulomb Attraction
electron and hole are treated independently
- Coulomb interaction added as a correction



$$E_{ehp}(n_h L_h n_e L_e) = E_g + \frac{\eta^2}{2a^2} \left\{ \frac{\varphi_{n_h, L_h}^2}{m_{eff}^v} + \frac{\varphi_{n_e, L_e}^2}{m_{eff}^c} \right\} - E_{coulomb}$$

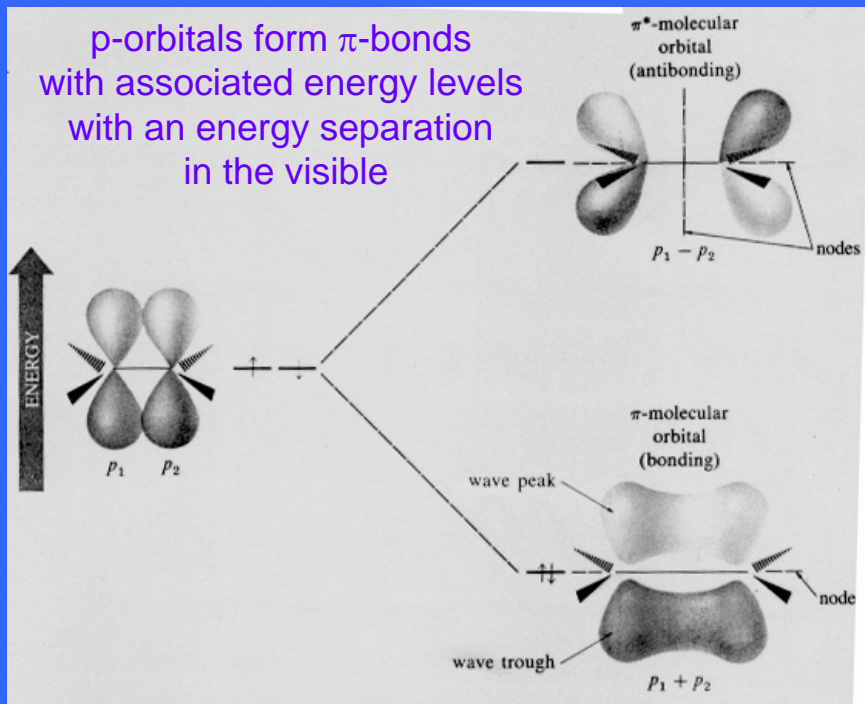
For $1S_e$ pairs of states $E_{coulomb} = 1.8e^2/\epsilon a$

Size Dependence of Electronic Structure



Development of Electronic Structure Similar to Length Dependence in 1D polyenes

p-orbitals form π -bonds with associated energy levels with an energy separation in the visible



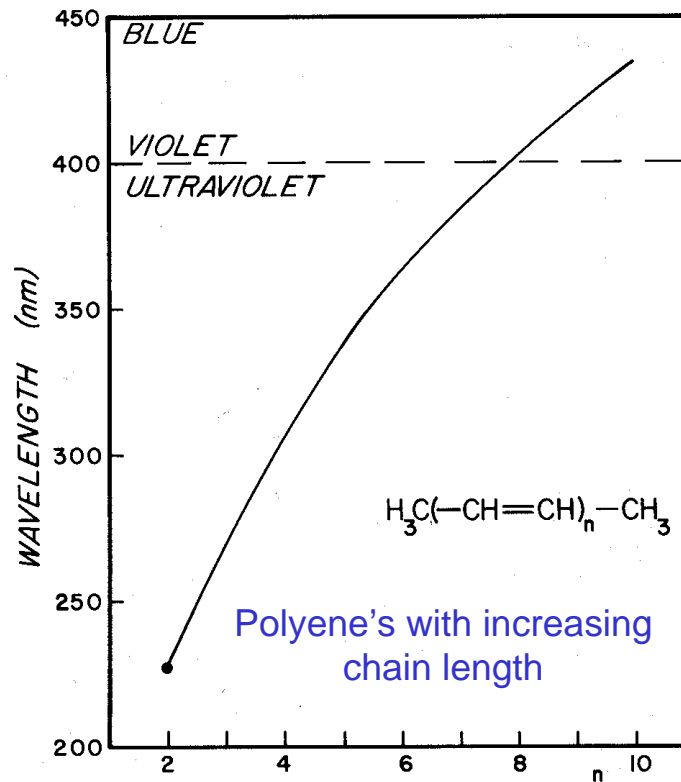
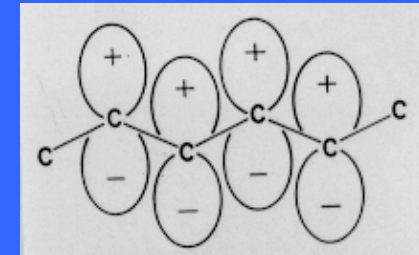
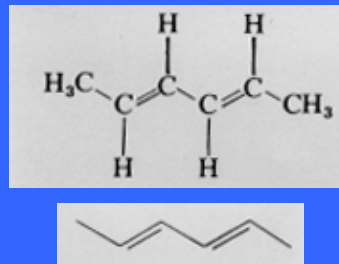
Lowest Unoccupied Molecular Orbital



Highest Occupied Molecular Orbital

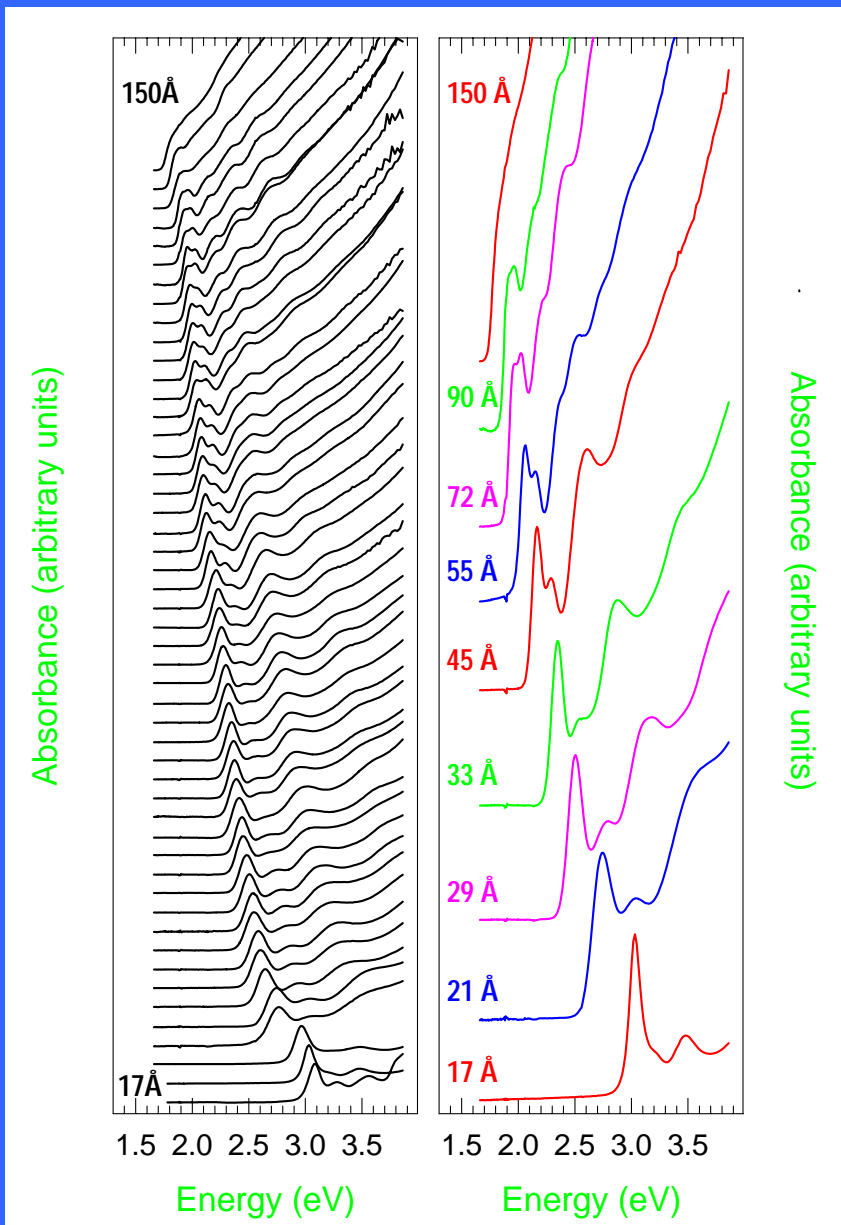


Example of alternating double/single bond π -bond extends over many C atoms

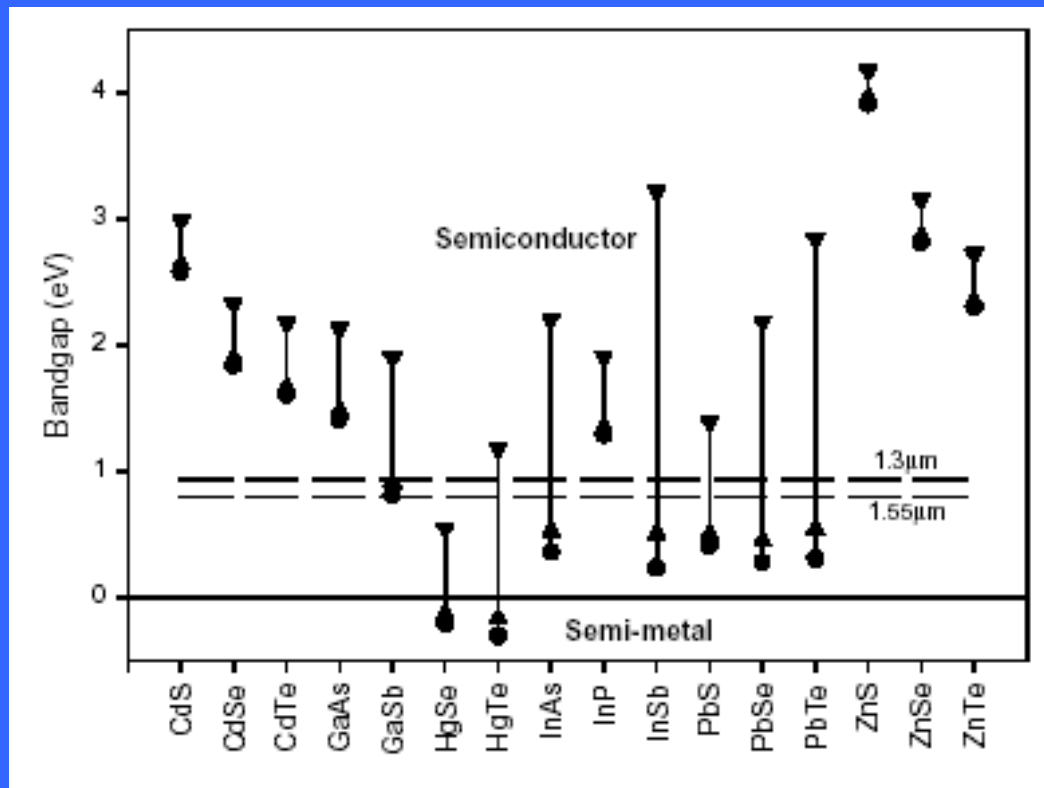


Size Dependent Absorption

Example: CdSe

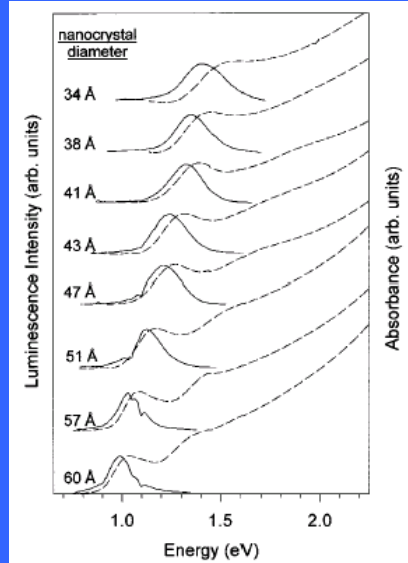


Semiconductor Materials

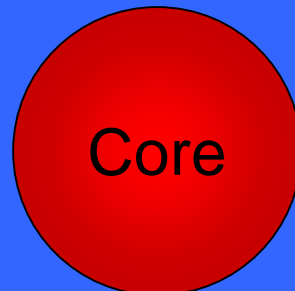


Range from 30 nm QDs to bulk crystal

Absorption Spectra of Semiconductor Nanocrystals



Changing the Core



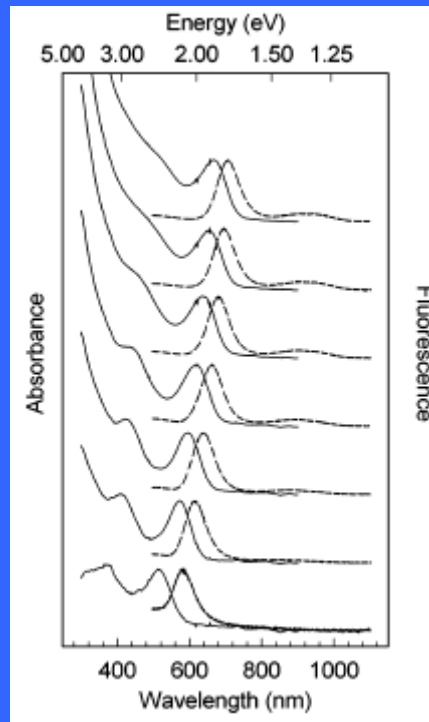
InAs

HgS

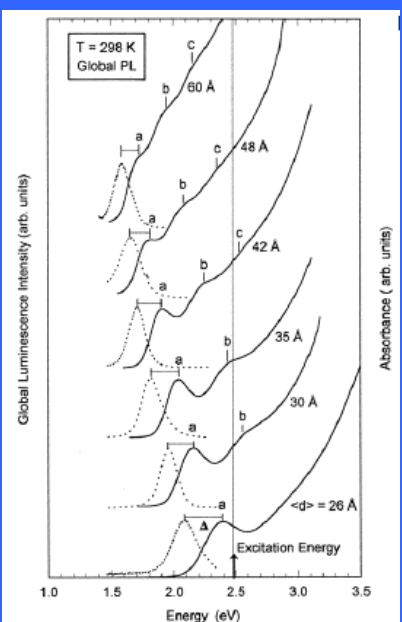
PbSe

PbS

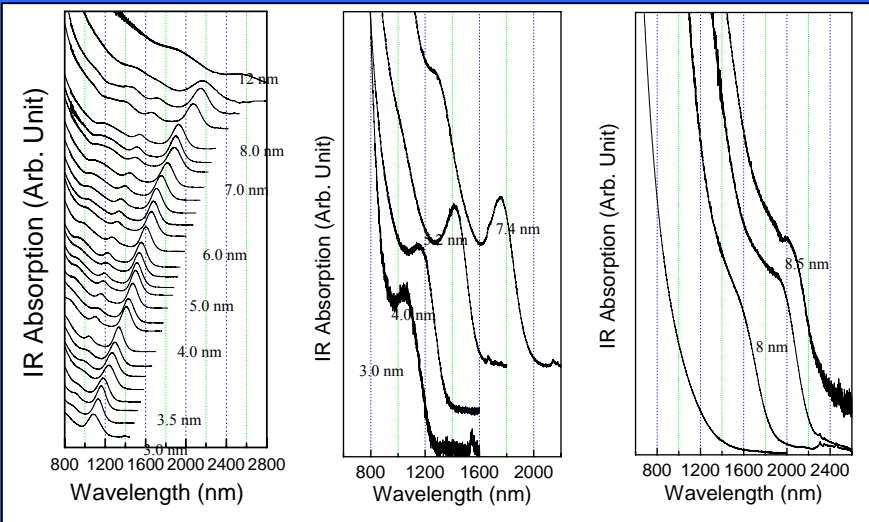
PbTe



A. P. Alivisatos, UC Berkeley



InP



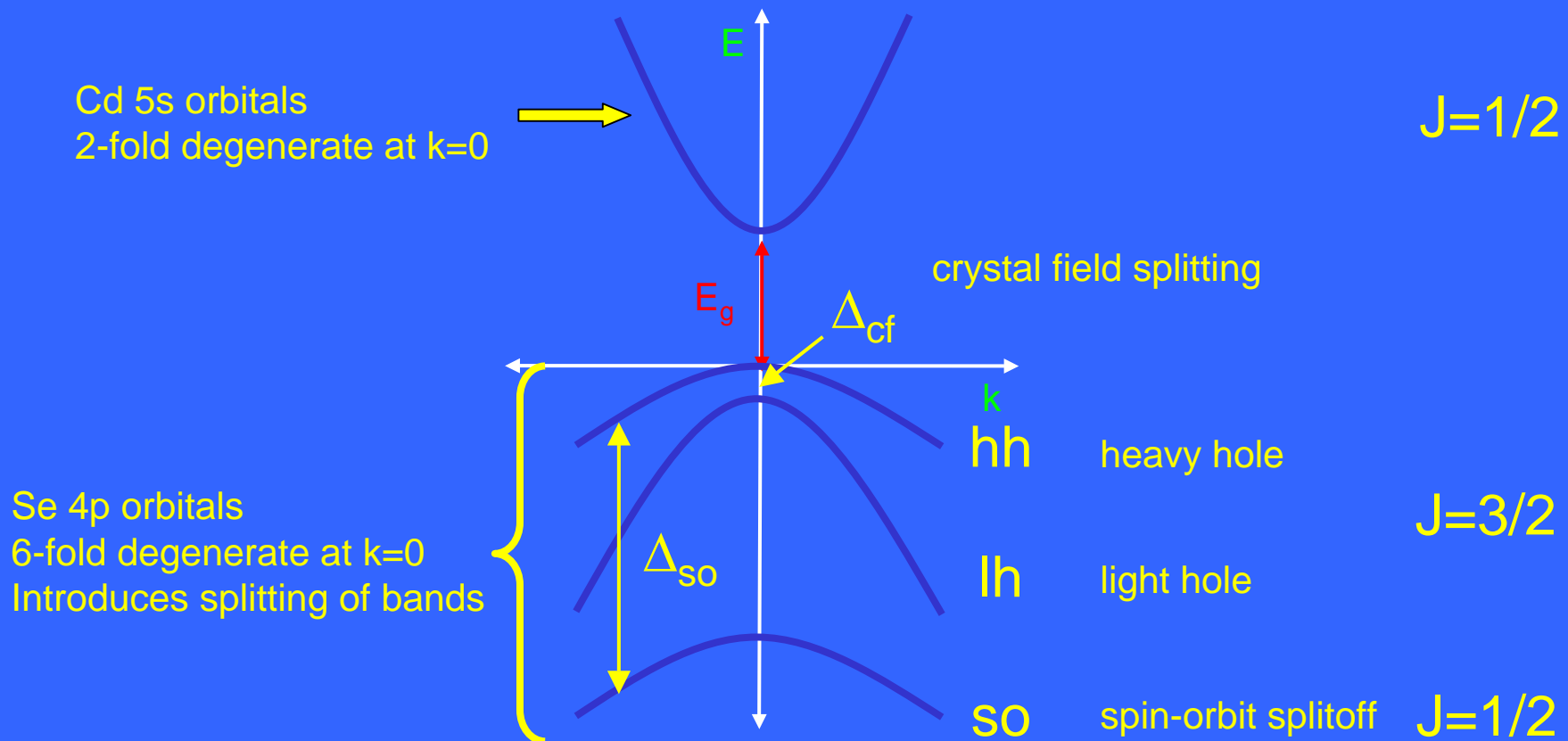
NRL group

O. Micic, A. Nozik, NREL

C. B. Murray, IBM

Real Band Structure

Example: CdSe

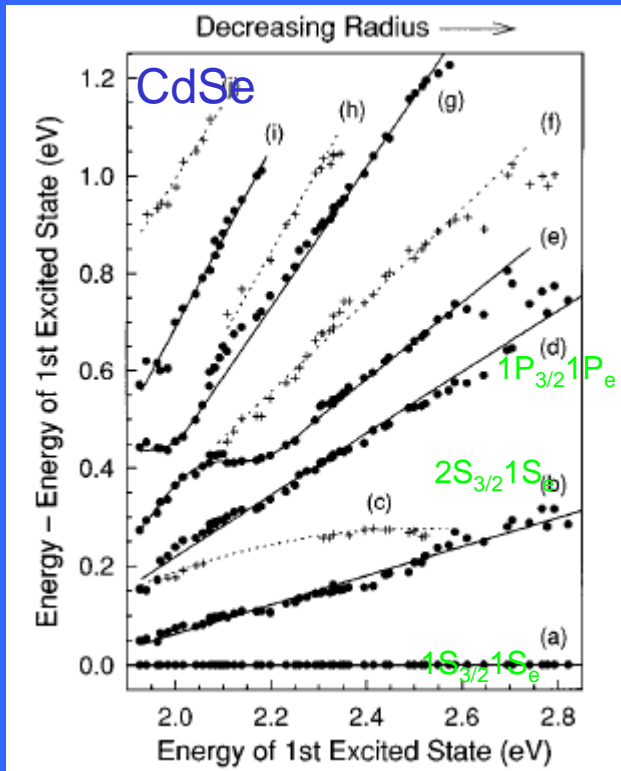


$$J = L + S$$

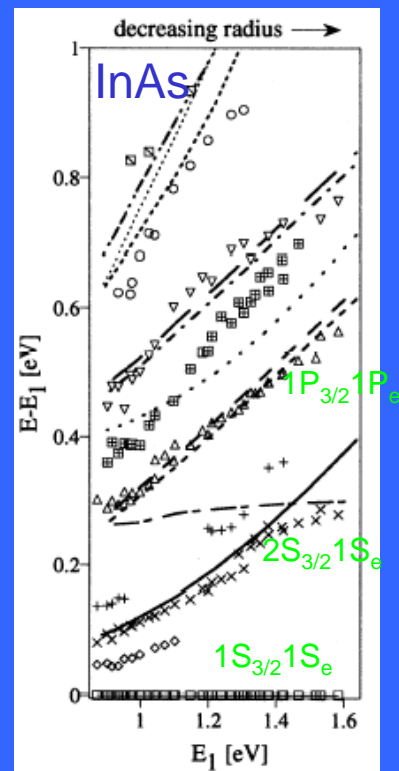
where L =orbital angular momentum
 S =spin angular momentum

J good quantum number due to strong spin-orbit coupling

Size Evolution of Electronic States



Low Band gap InAs modeling must also account for valence-conduction band coupling



D. J. Norris, M. G. Bawendi, Phys. Rev. B **53**, 16338 (1996).

U. Banin et al., J. Chem. Phys. **109**, 2306 (1998).

$F = J + L$ where L =envelope angular momentum
 J =Bloch-band edge angular momentum

Hole states labeled by $n_h L_F$ [$L_F = L + (L+2)$]
 Electron states labeled $n_e L_e$

Selection Rules

$$P = \left| \langle \Psi_e | \hat{e} \cdot \hat{p} | \Psi_h \rangle \right|^2$$

polarization
vector of light

momentum
operator

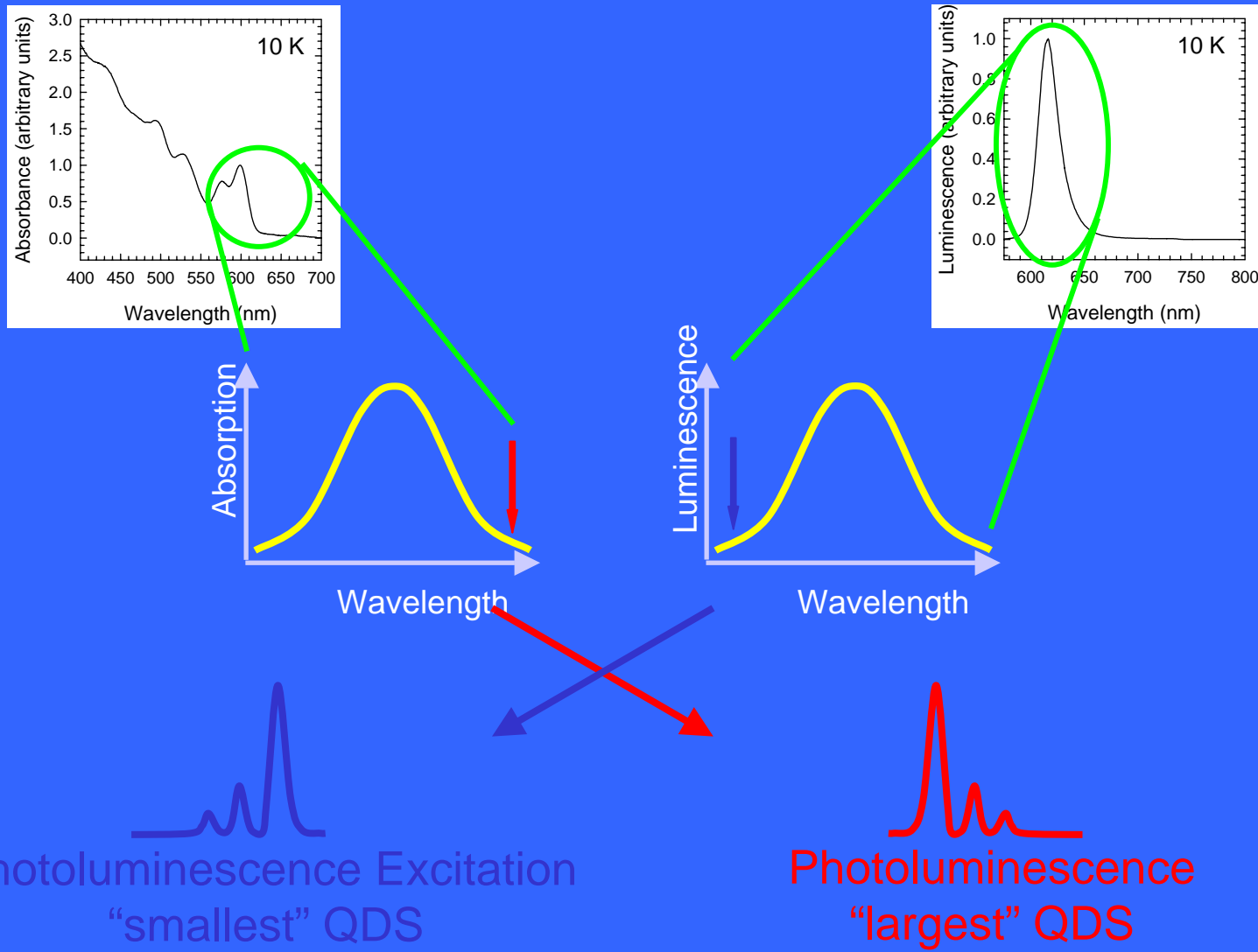
acts only on unit cell
portion of wavefunction

$$P = \left| \langle u_c | \hat{e} \cdot \hat{p} | u_v \rangle \right|^2 \left| \langle f_e | f_h \rangle \right|^2$$

$$P = \left| \langle u_c | \hat{e} \cdot \hat{p} | u_v \rangle \right|^2 \delta_{n_e, n_h} \delta_{L_e, L_h}$$

Overlap of the electron and hole wavefunctions within the QDs

Towards the Homogeneous Distribution: Photoluminescence and Photoluminescence Excitation

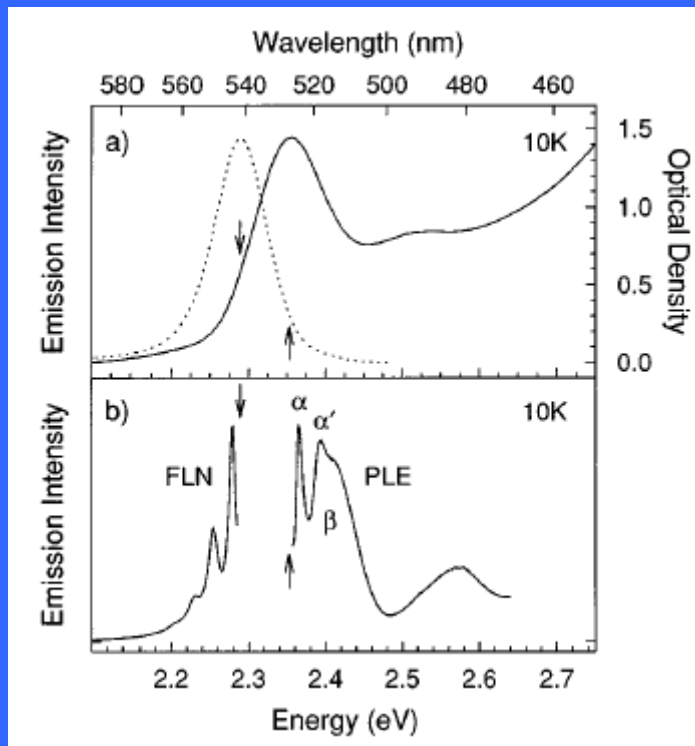


Photoluminescence Excitation
“smallest” QDS

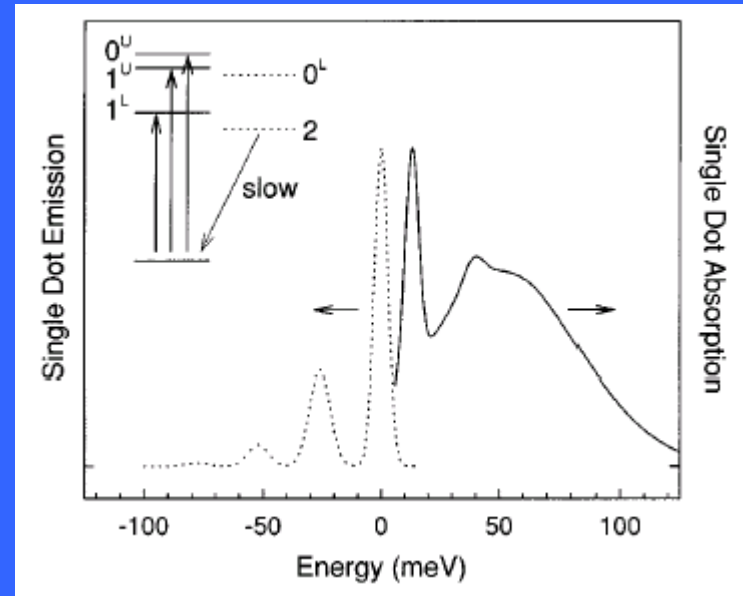
Photoluminescence
“largest” QDS

Distribution in ensemble from size, structure, and environmental inhomogeneities

Fluorescence Line Narrowing and Photoluminescence Excitation

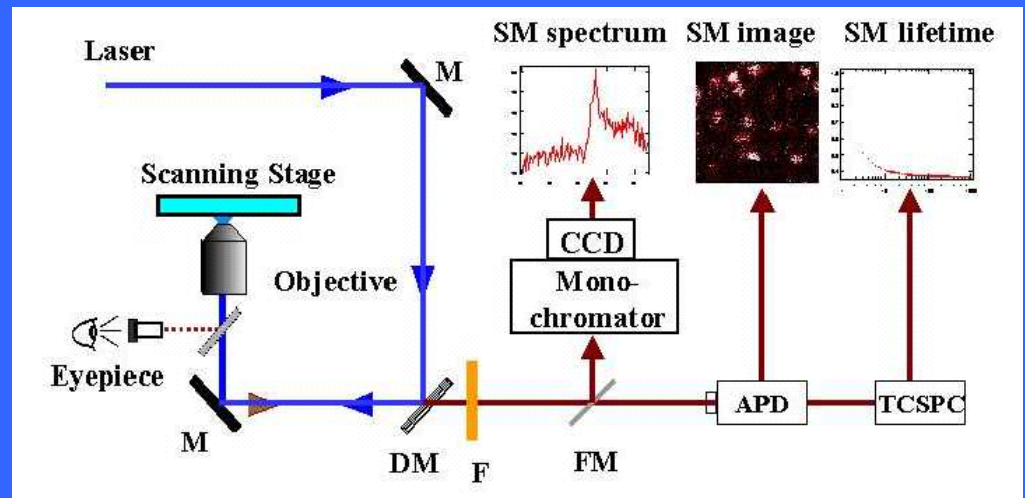
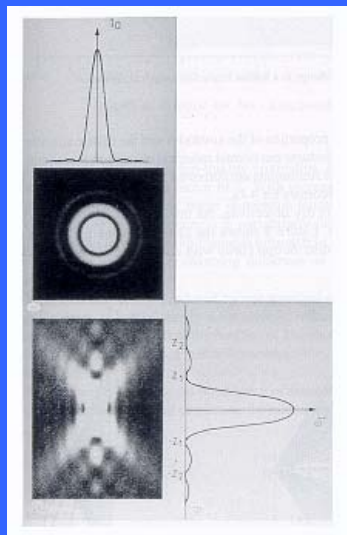


Band Edge Exciton Structure



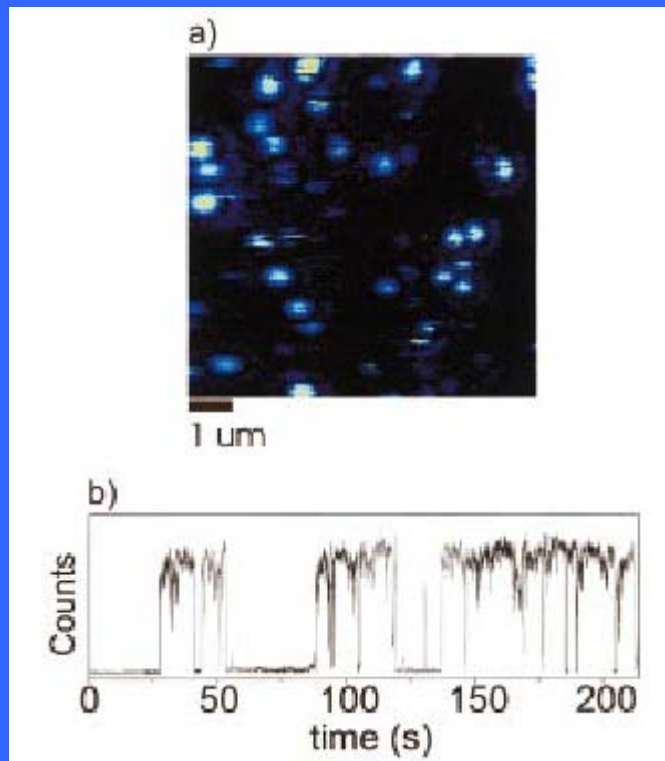
Splitting due to crystal field, non-spherical shape, and exchange interactions of quantum dots

Single Molecule Spectroscopy



Diffraction Limited Spot

Fluorescence Intermittancy in CdSe QDs



QDs “blink” like molecules

On-period decreases with increasing illumination intensity

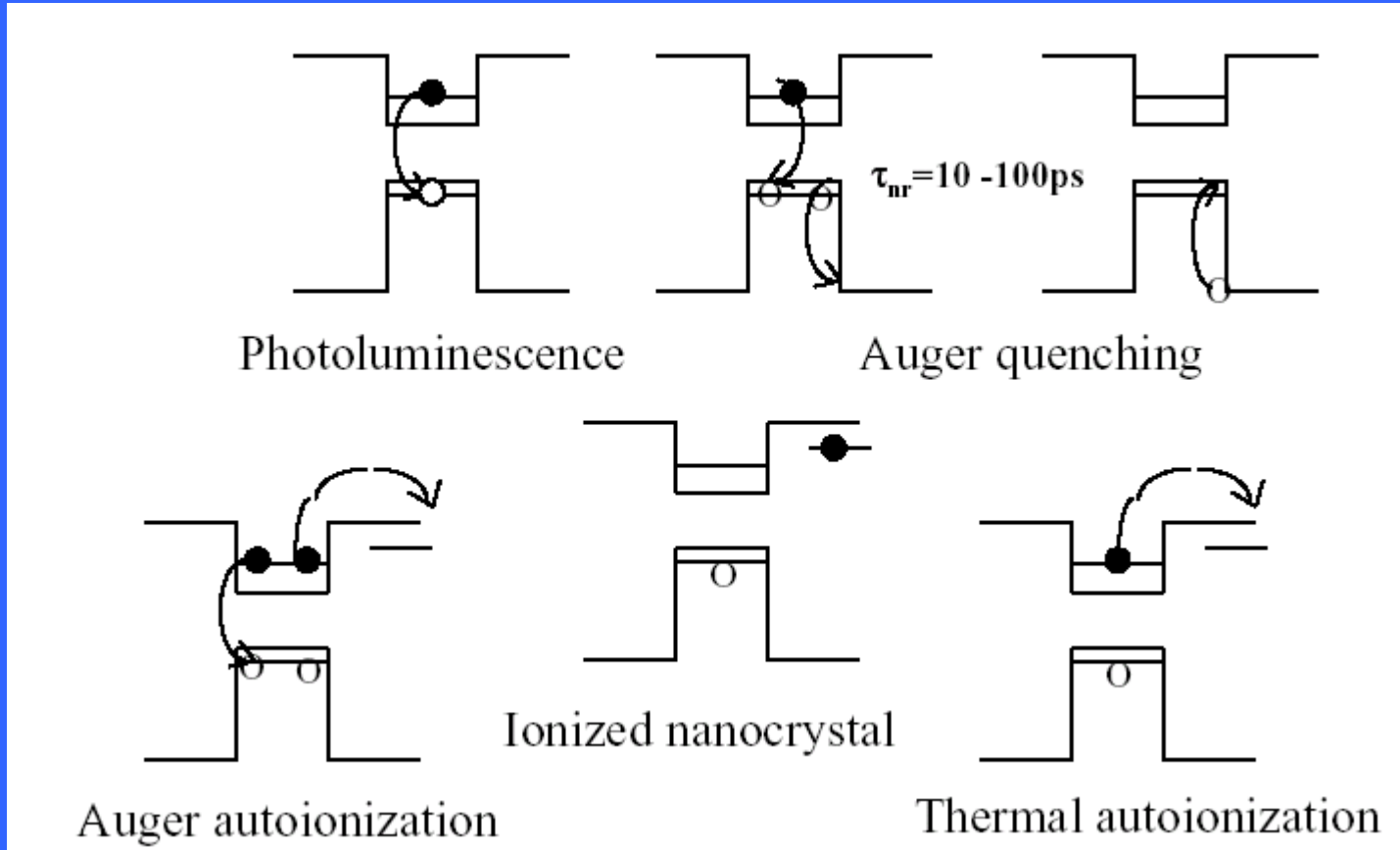
Off-period intensity independent

Excitation every 10^{-5} sec
Relaxation every 10^{-8} sec

But occasionally
Two electron-hole pairs may
exist in a single QD

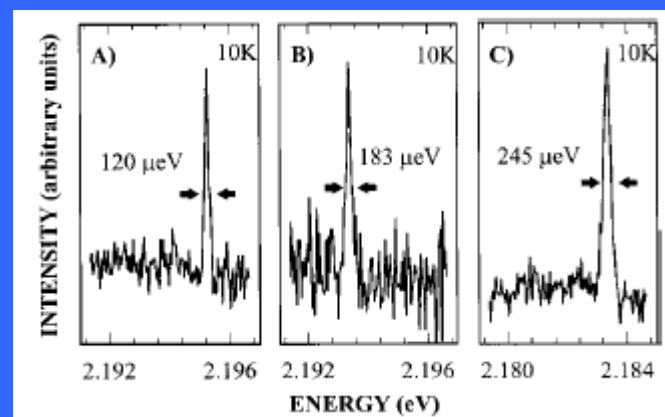
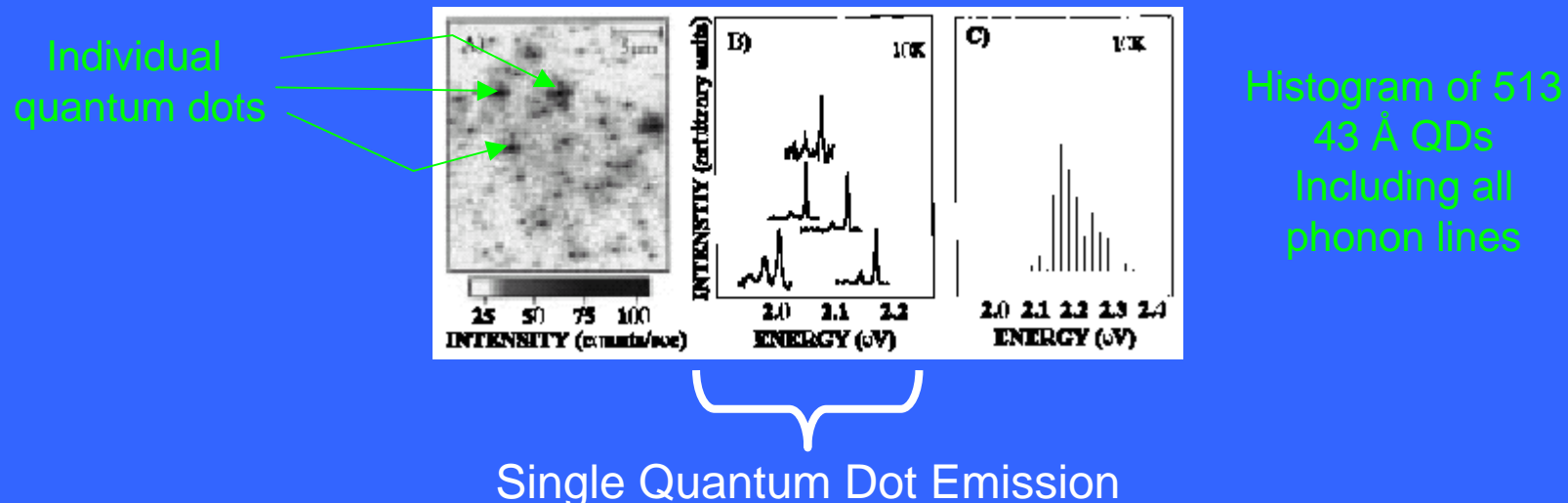
 Auger ionization
Probability of photoionization/excitation 10^{-6}
Neutralization time ~0.5 sec

Auger ionization

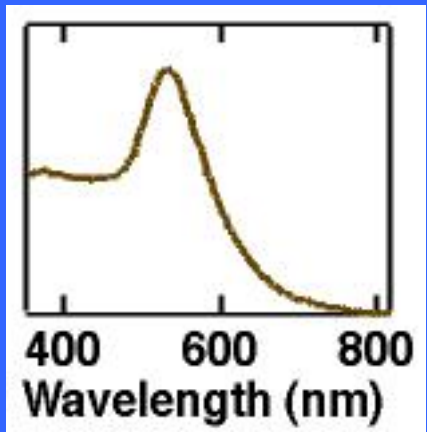
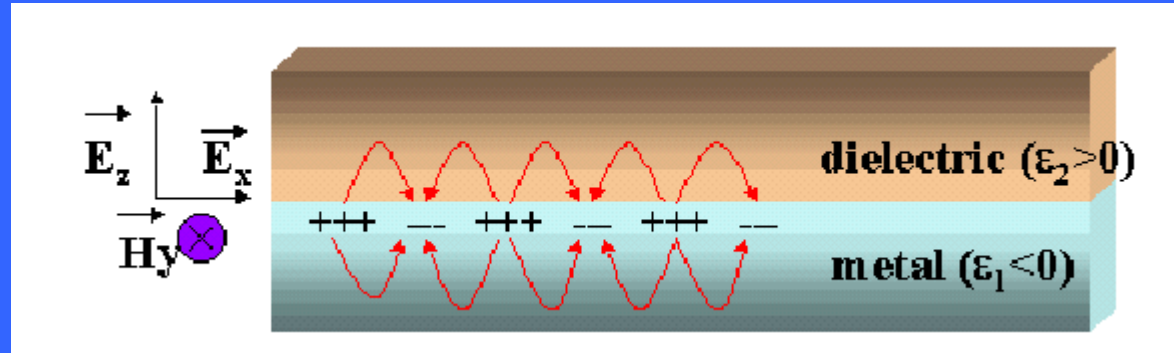
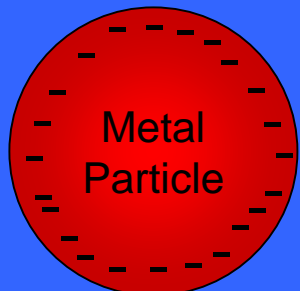


Consistent with single molecule spectroscopy and photodarkening
observed in QD doped glasses

Single Dot Spectroscopy



Metal Nanoparticles

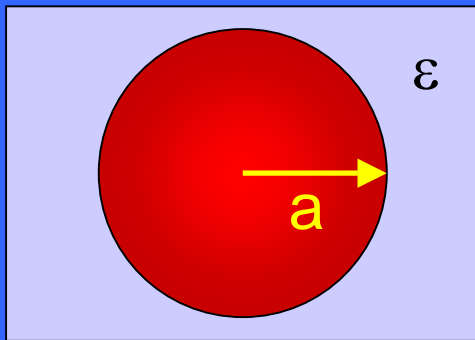


Au nanoparticle
absorption

Surface Plasmon Resonance

- dipolar, collective excitation between negatively charge free electrons and positively charged core
- energy depends on free electron density and dielectric surroundings
- resonance sharpens with increasing particle size as scattering distance to surface increases

Electronic Properties of Semiconductor and Metal Nanoparticles



Charge not completely solvated
as in infinite solid

Nanoparticle capacitance

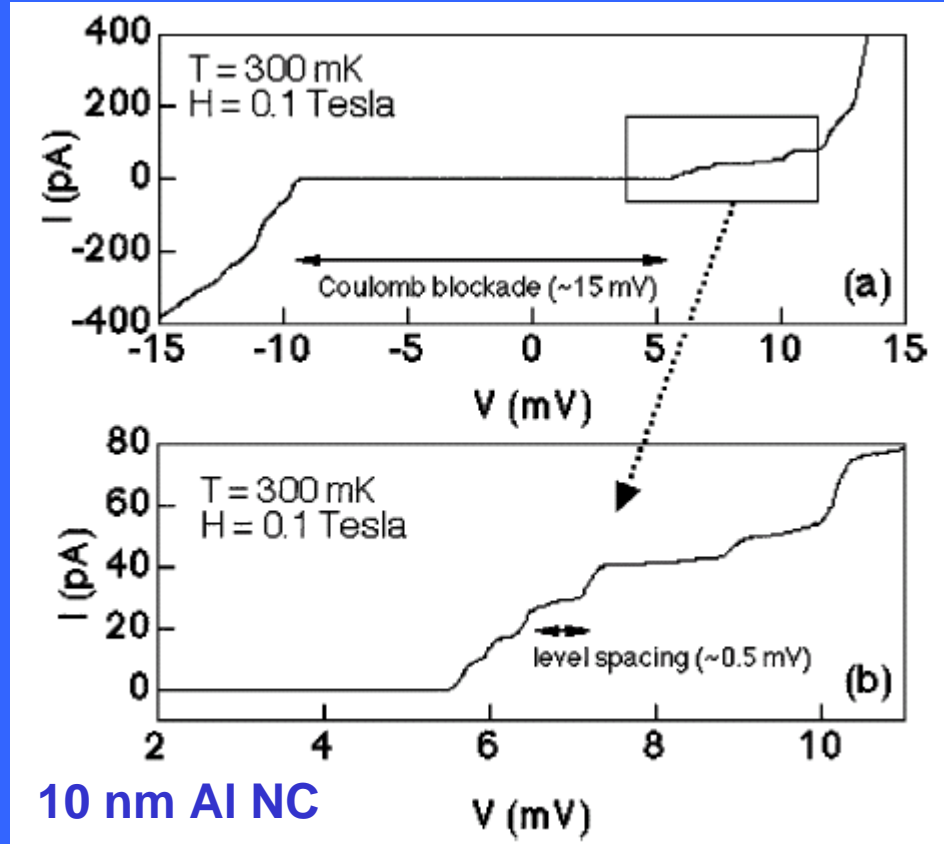
$$C = 4\pi\epsilon_0\epsilon a$$

Charging Energy

$$E_c = \frac{e^2}{2C(a)}$$



Coulomb blockade at
 $k_B T < E_c$

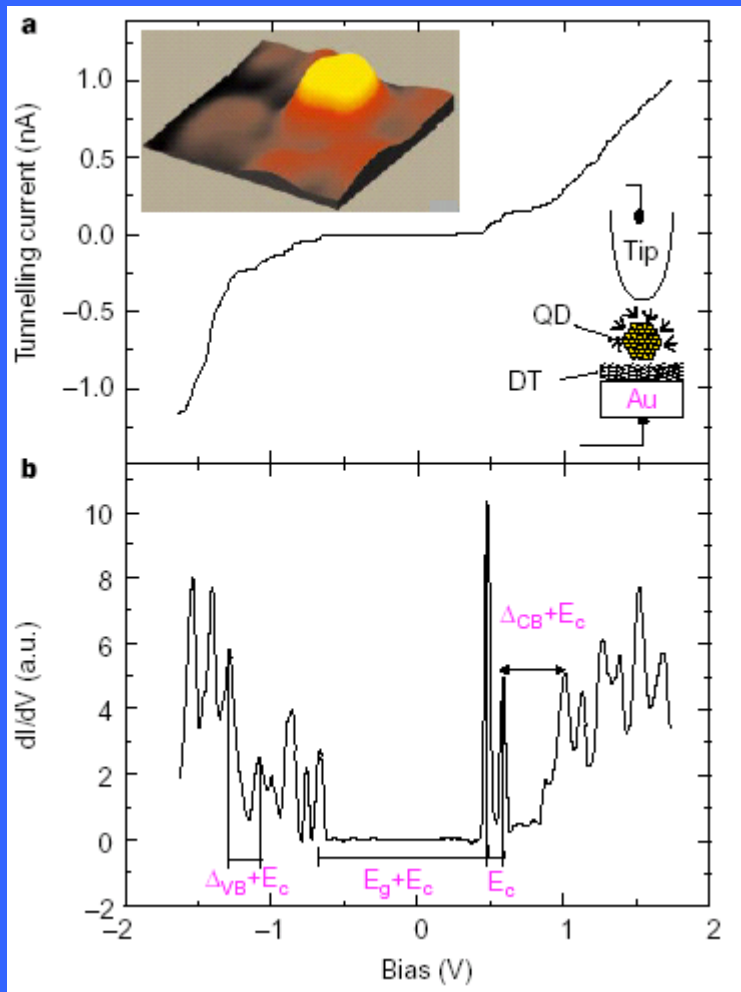


Courtesy of C. T. Black, Thesis, Harvard U.

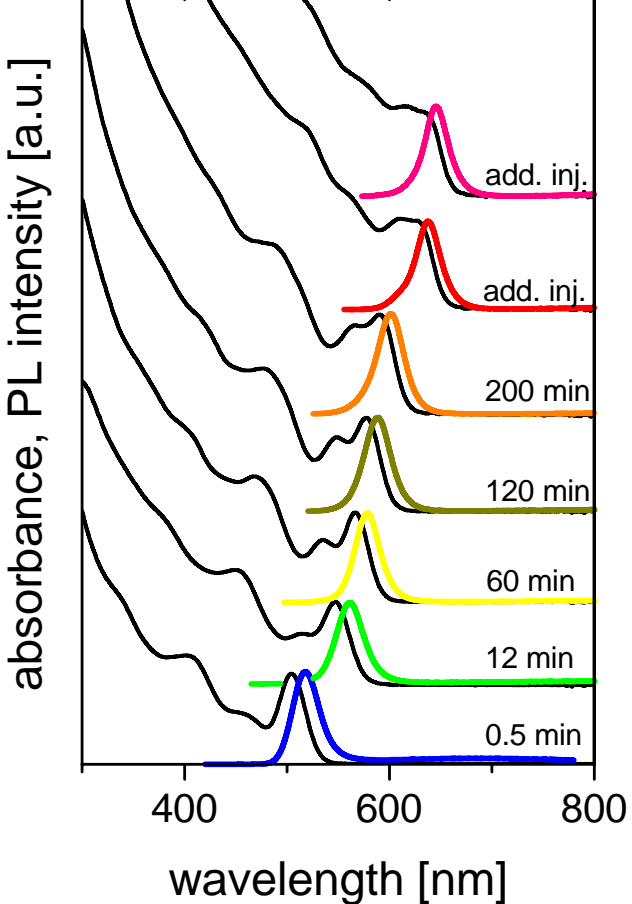
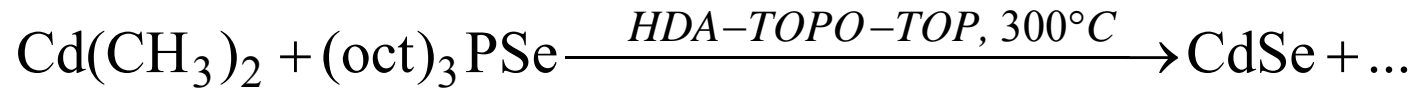
Structure from discrete electronic states of
metal NC

STM Measurements on Single QDs

InAs QDs

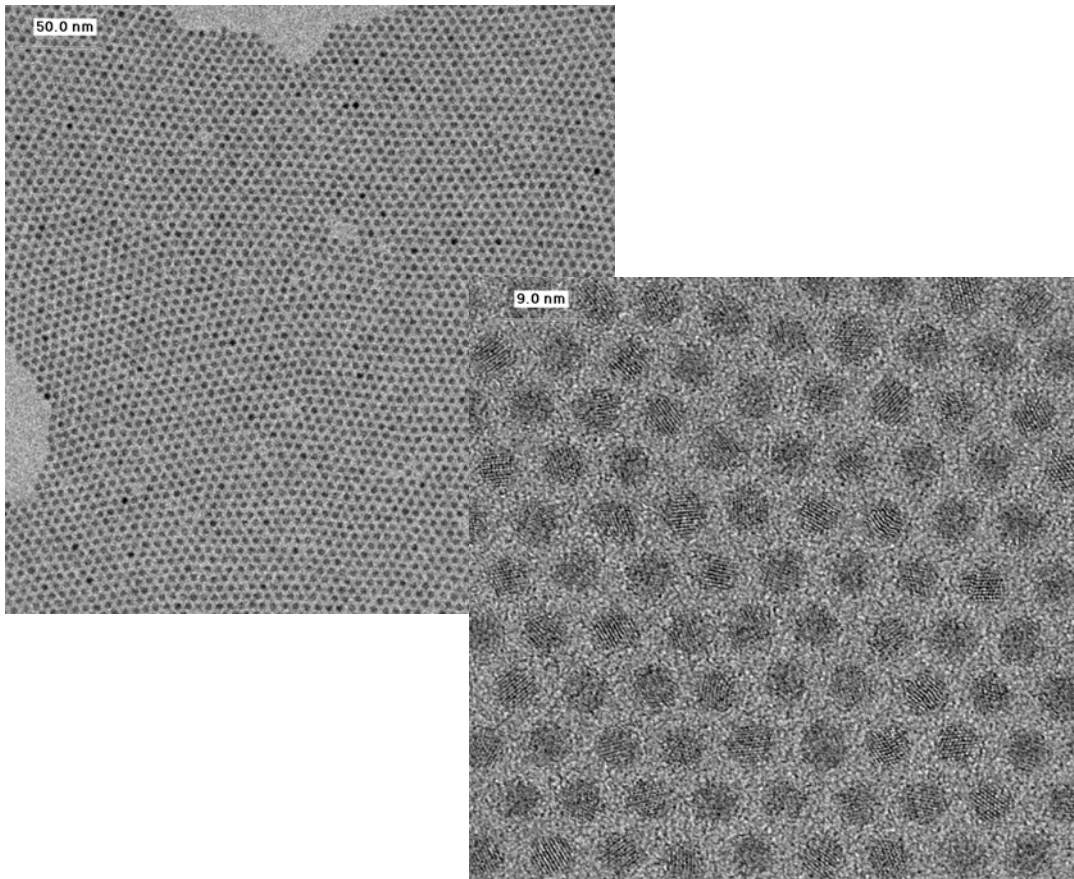


Synthesis of monodisperse CdSe nanocrystals



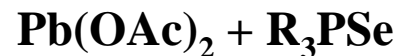
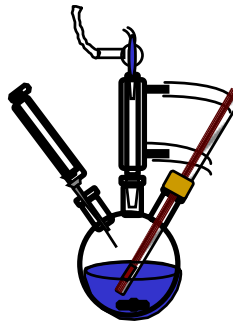
UV-Vis and PL spectra of CdSe nanocrystals in growth at 300°C

TEM and HRTEM images of as-prepared CdSe nanocrystals.



Wet Chemical Synthesis of PbSe Nanocrystals and Superlattices

Synthesis

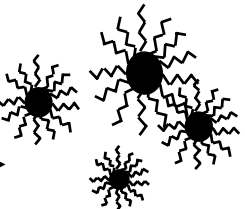


oleic acid,

R_3P , T=150 C

PbSe

R= octyl

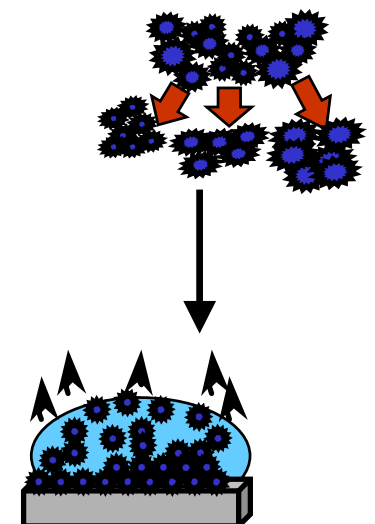
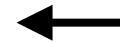
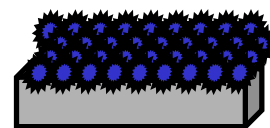


Size Selective Processing

Size selective precipitation in solvent/ non solvent pairs like hexane-methanol

Self Assembly

Evaporation of the solvent

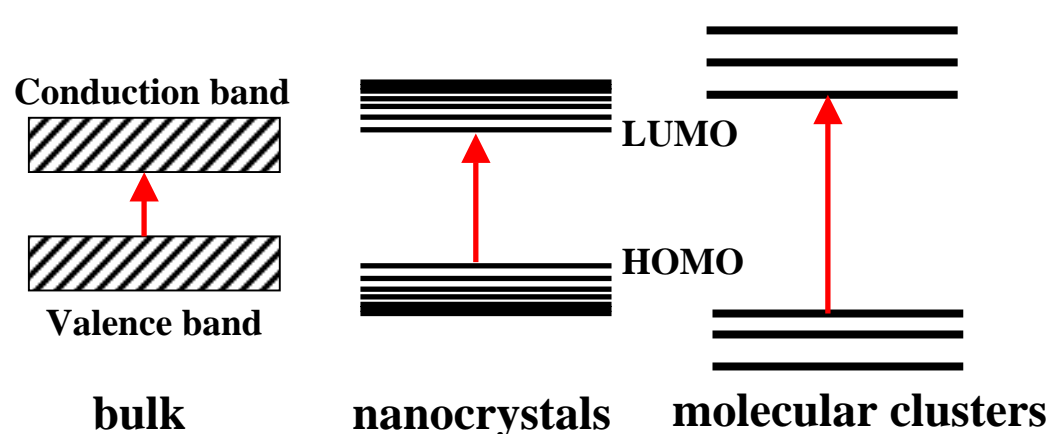


PbSe Nanocrystals and Nanowires

Nanocrystals:

1.5 – 10 nm diameters

100 – 100 000 atoms



PbSe Nanocrystal

Small Bandgap (0.28 eV, cf CdSe : 1.70 eV) \Rightarrow IR detector, IR diode Laser Material

Larger Bohr Radius (PbSe 46 nm, CdSe 12nm) \Rightarrow Strong Confinement of Electron-Hole Pair

Larger Optical Nonlinearity, Thermoelectric Cooling ($ZT = 1$: PbTe)

Semiconducting, Solar Cells, Thermoelectric, Biological Application

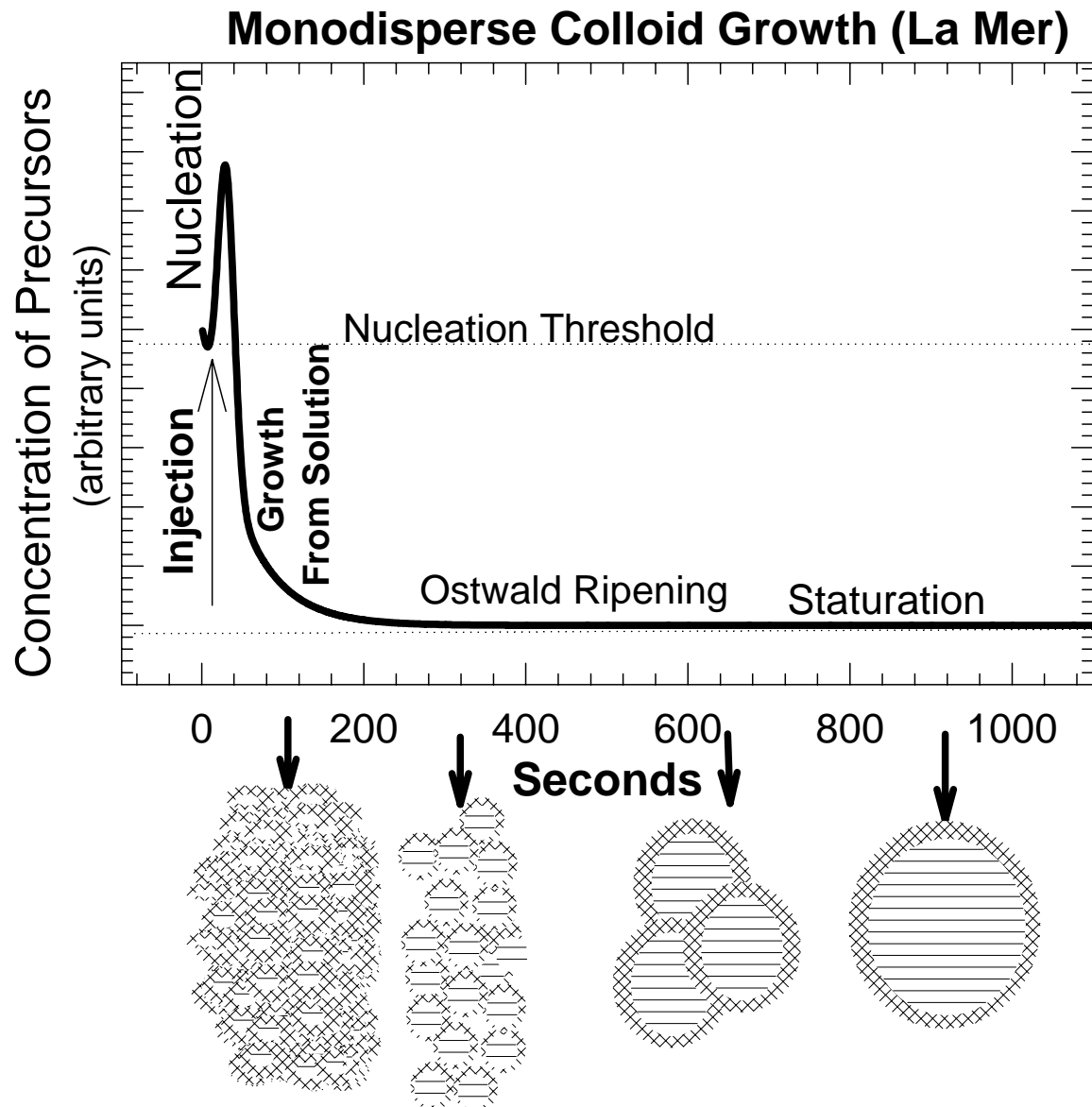
PbSe Nanowire

Solution Phase Synthesis using the Nanoparticles as a Building Block

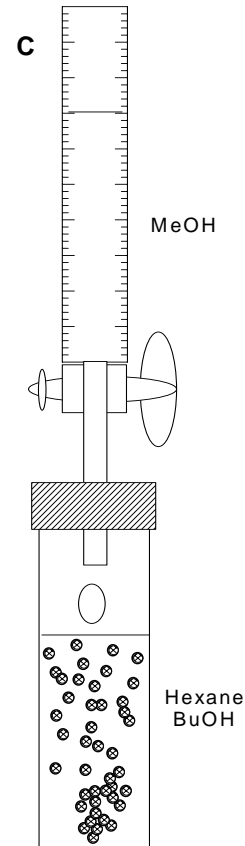
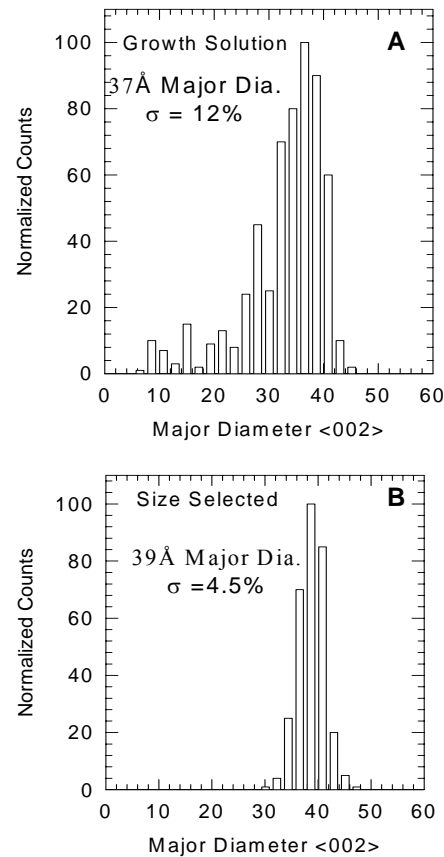
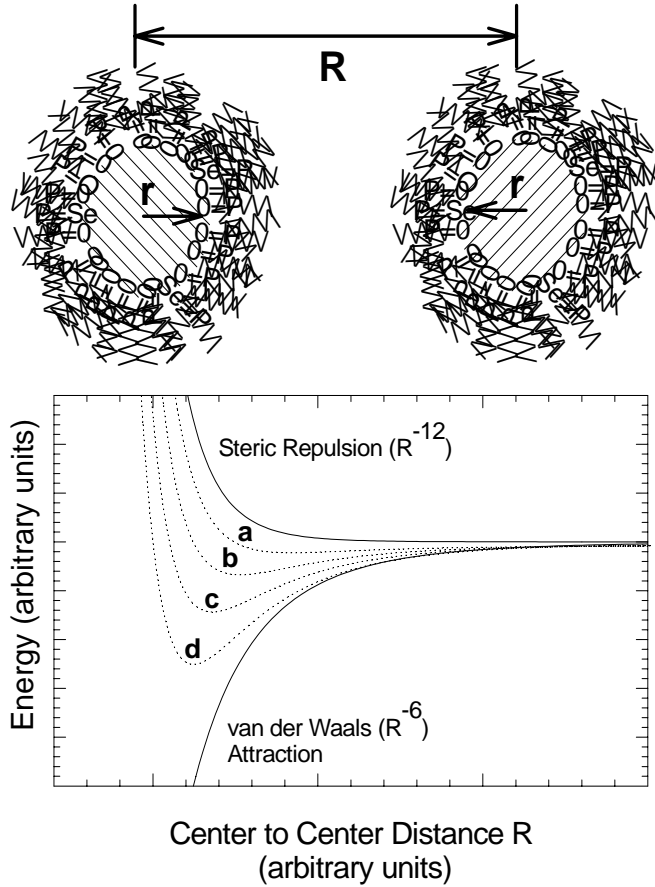
Formation of the Nanowires from the Self Assembling the Particles

Controlling the wire Properties by Changing the Size and Shape of the Particles

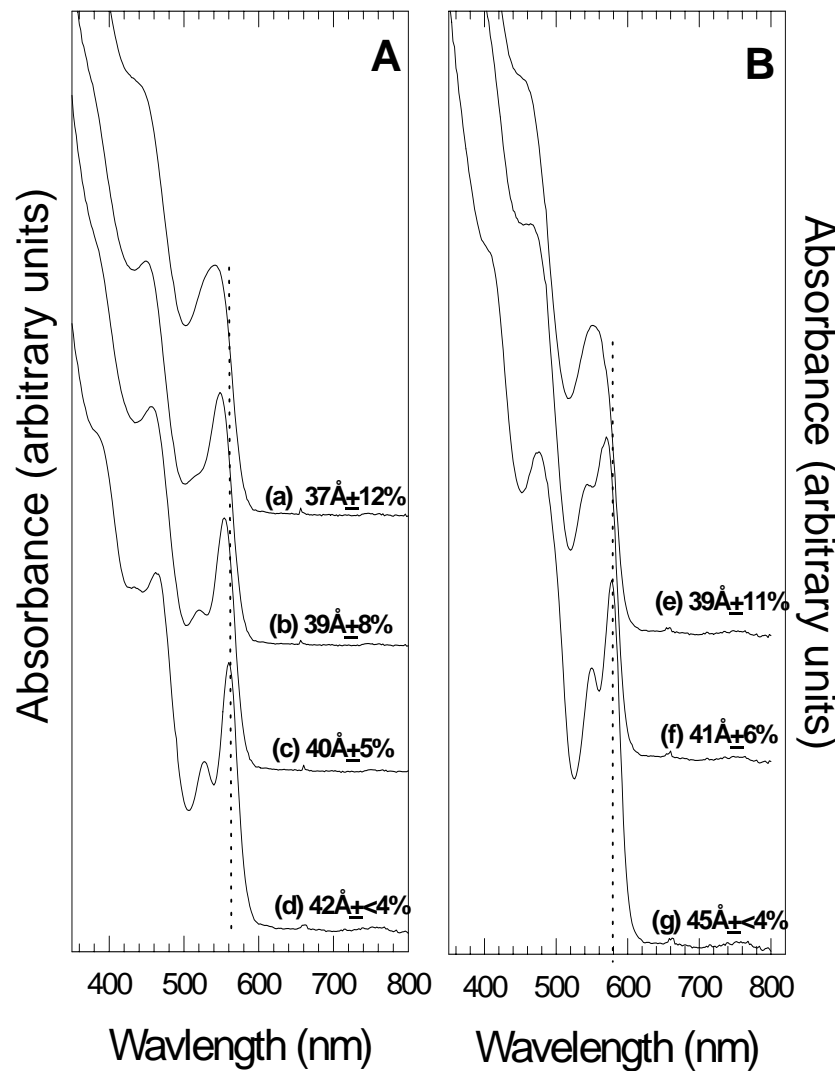
Semiconducting device, Interconnect, Building Blocks for the Nanodevice

A

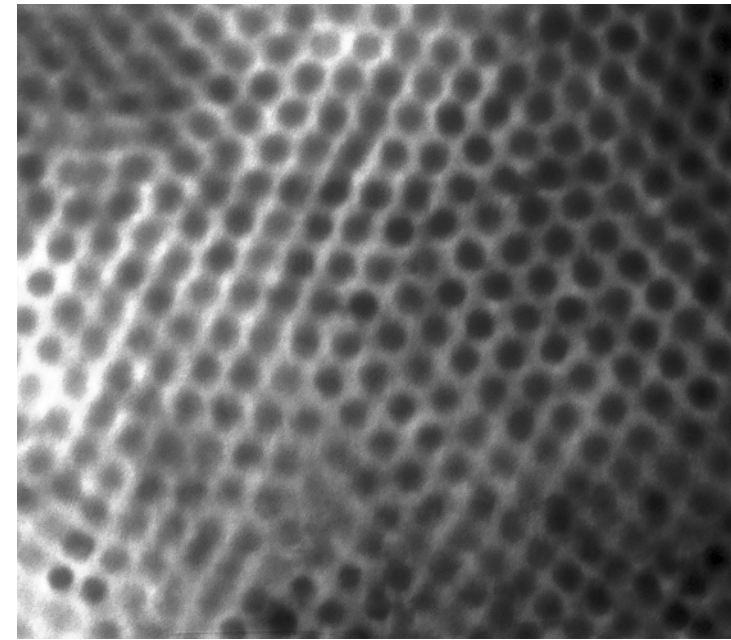
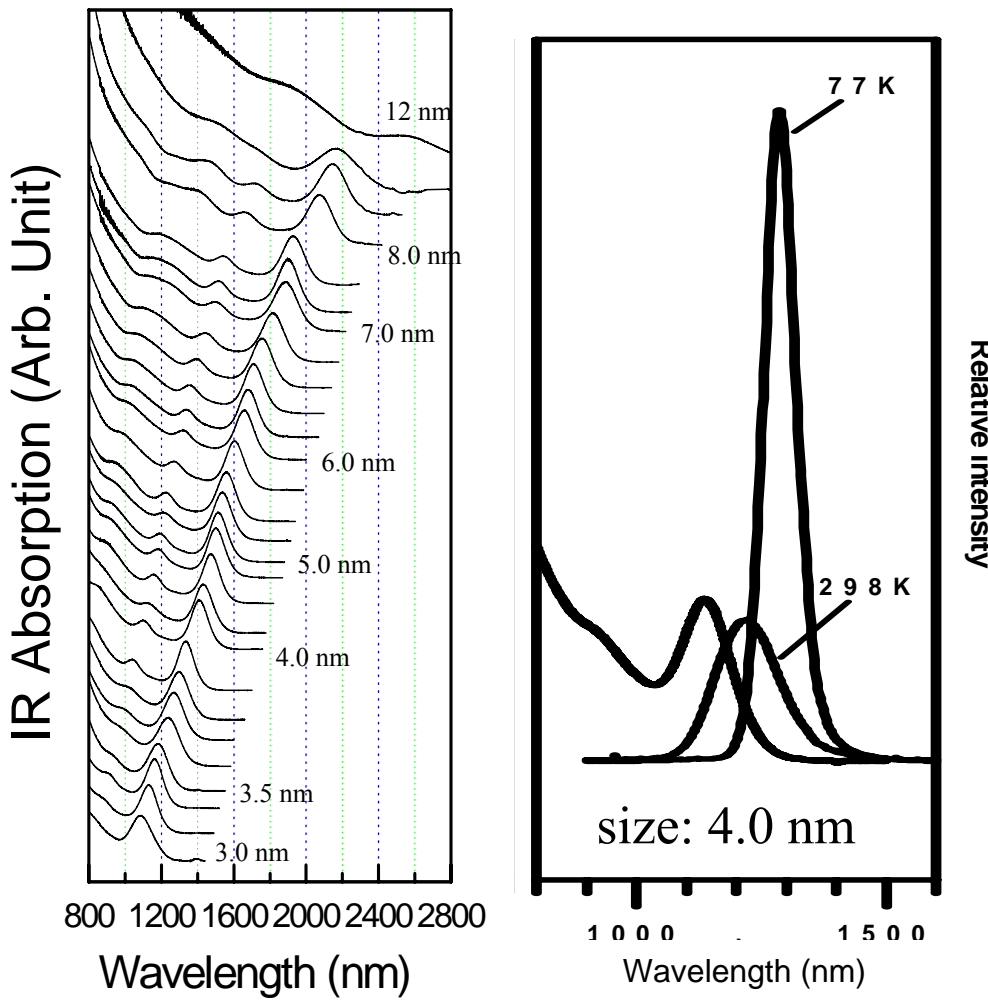
Size selective processing:



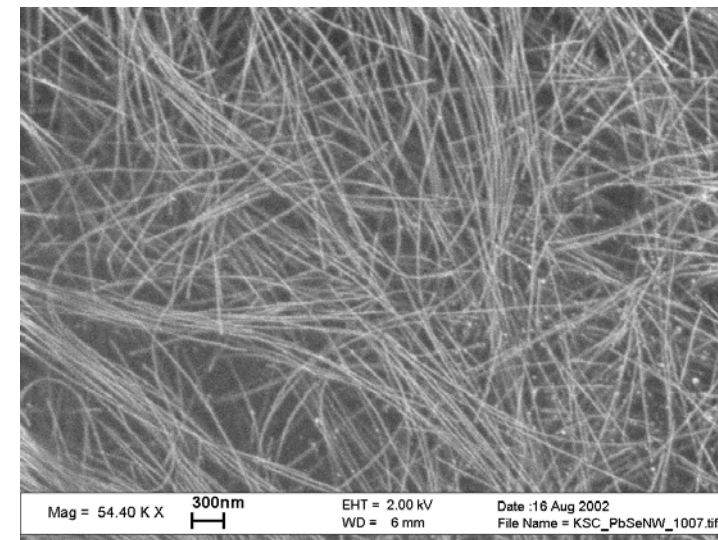
Results of size selected Percipitation



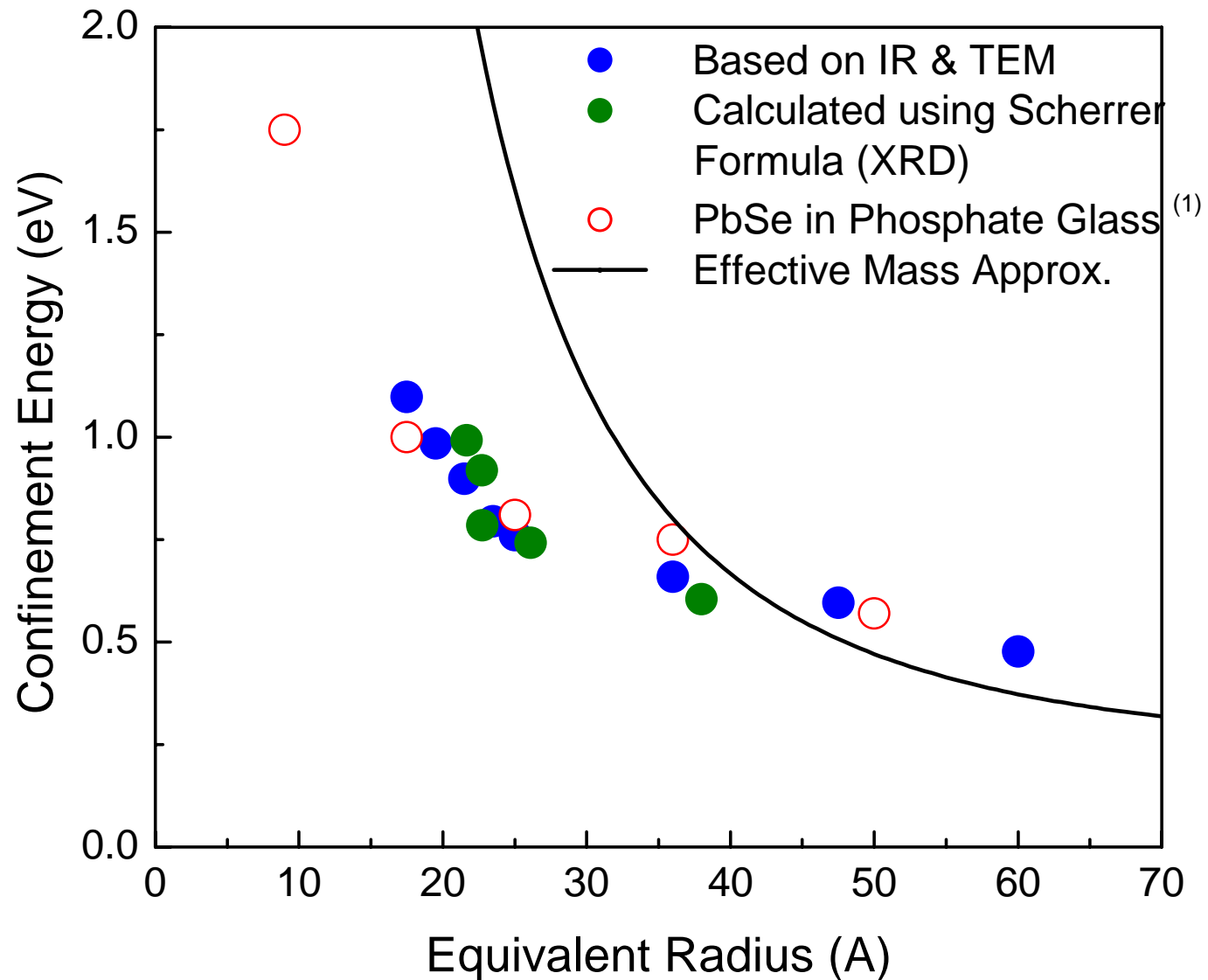
Absorption and Photoluminescence of PbSe Nanocrystals



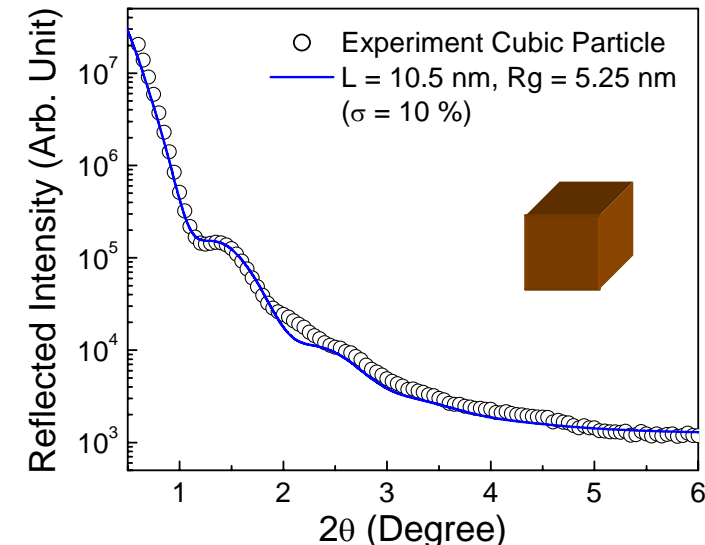
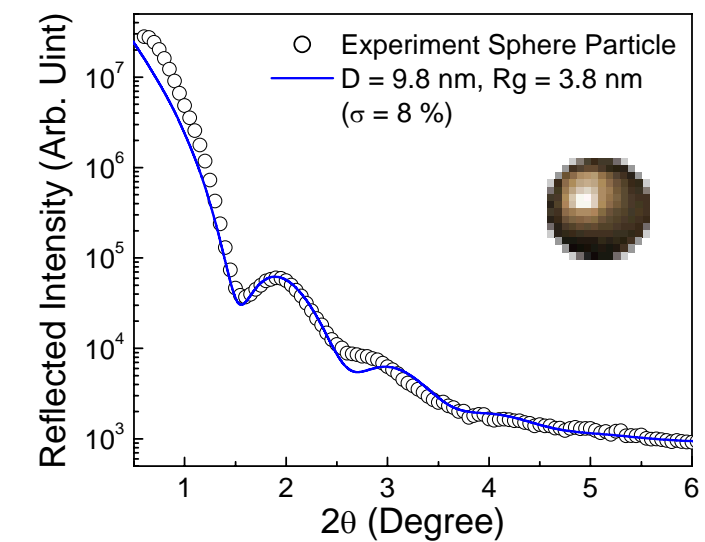
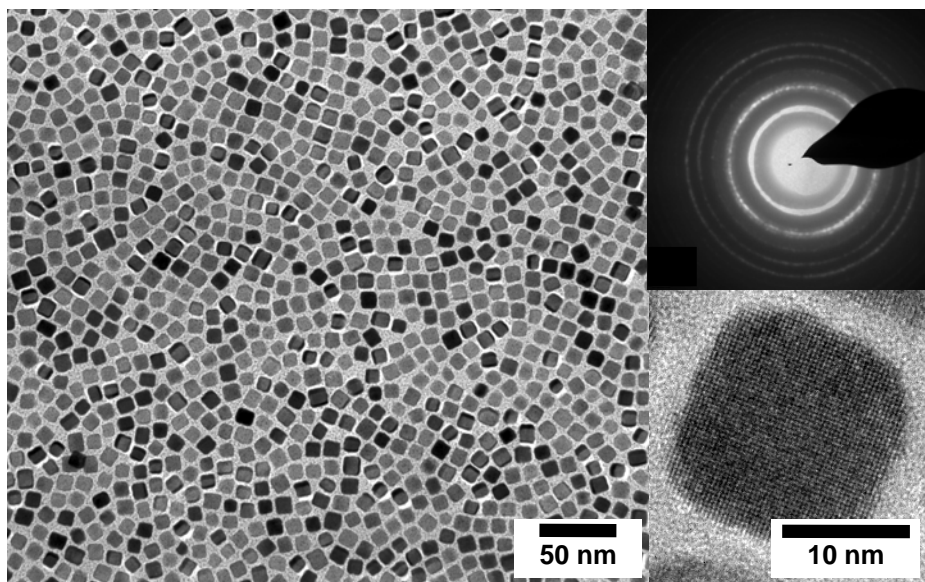
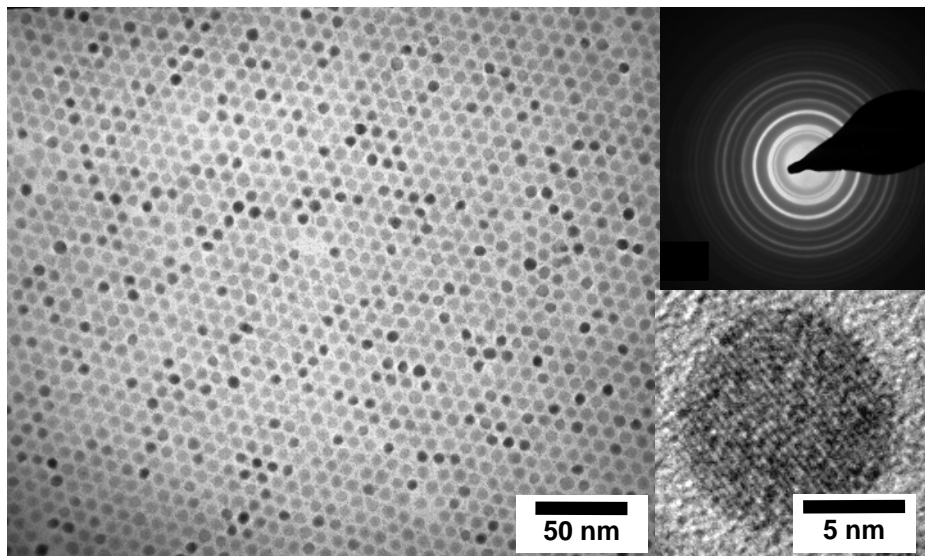
PbSe Nanocrystals



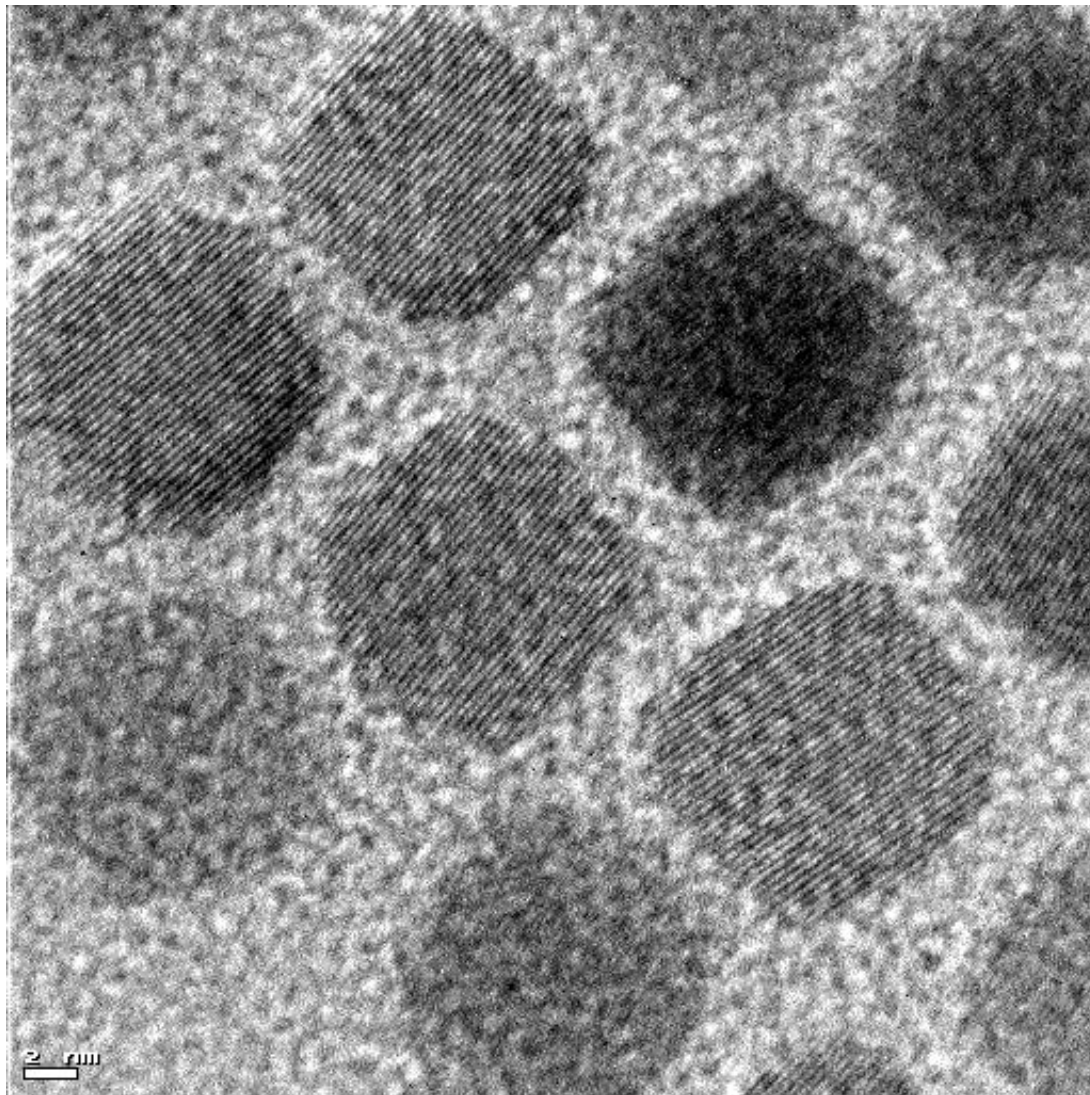
PbSe nanowires

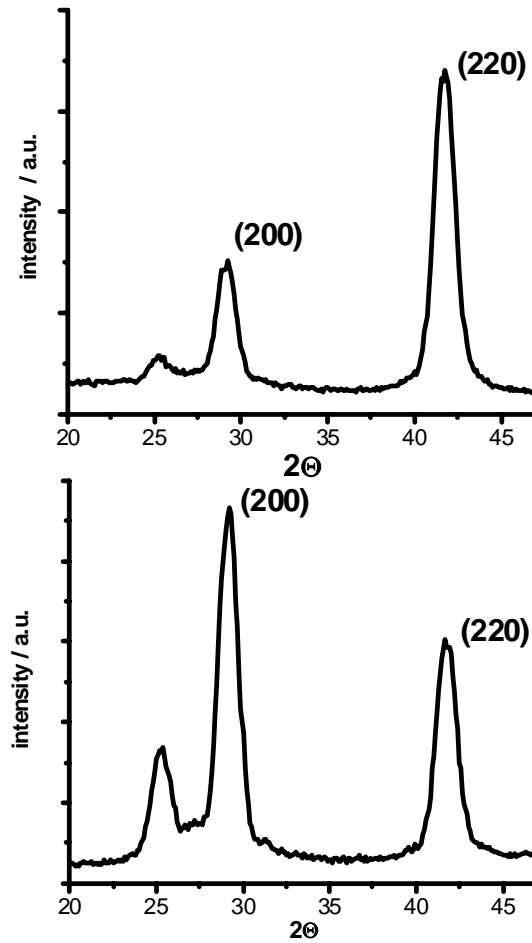
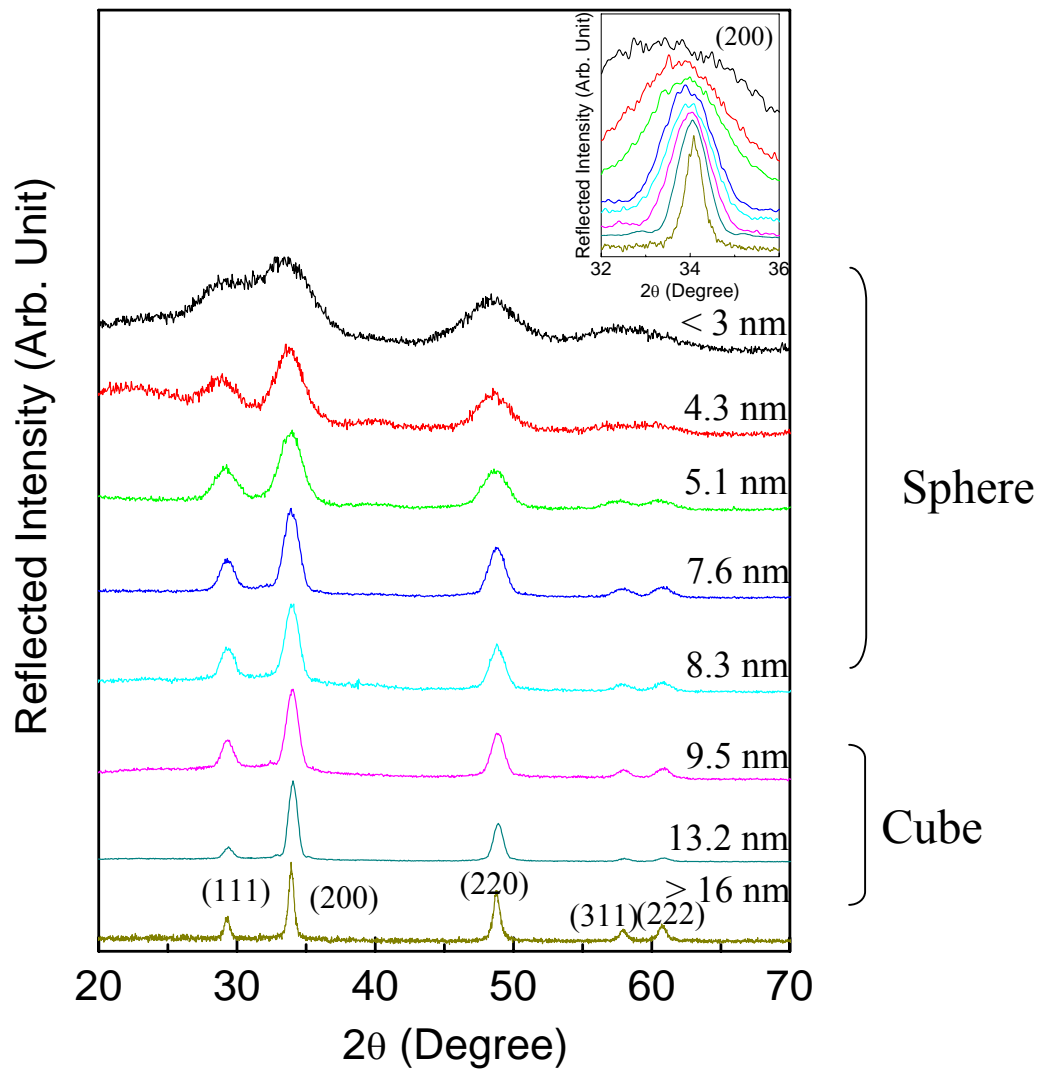


Shape Change from Sphere to Cubic and SAXS in Polymer Matrix



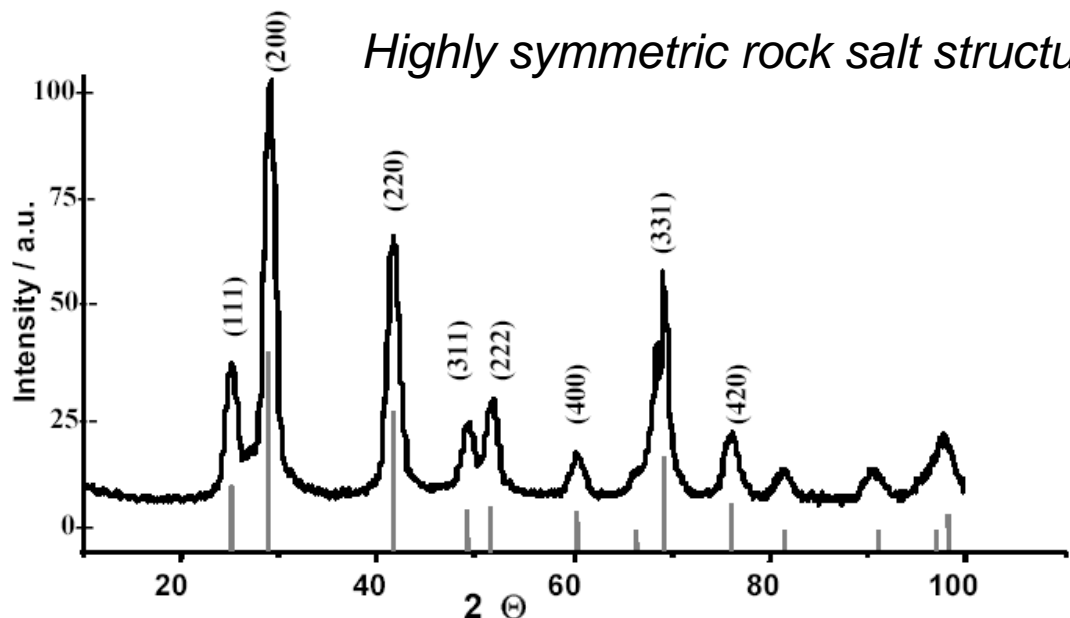
PbSe Quantum Cubes



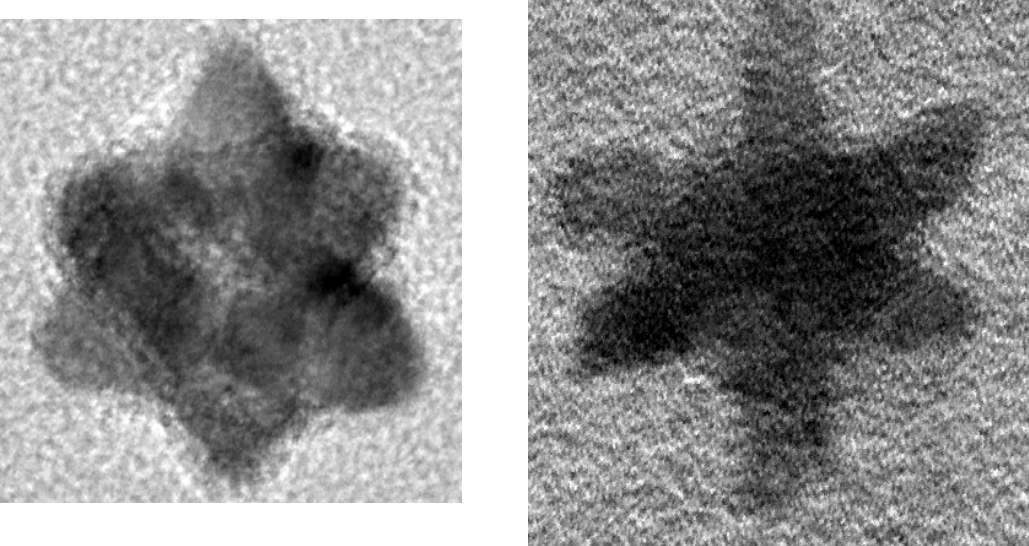
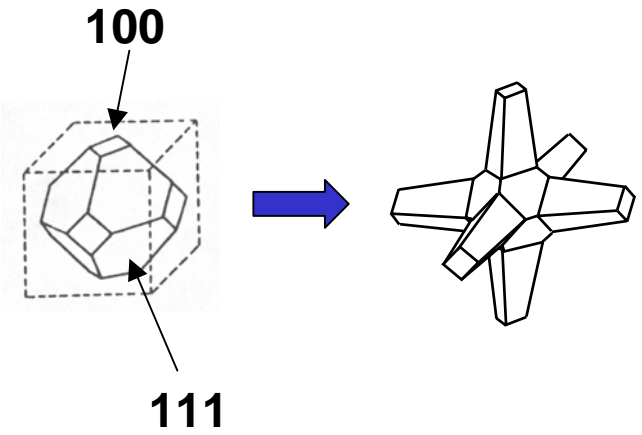
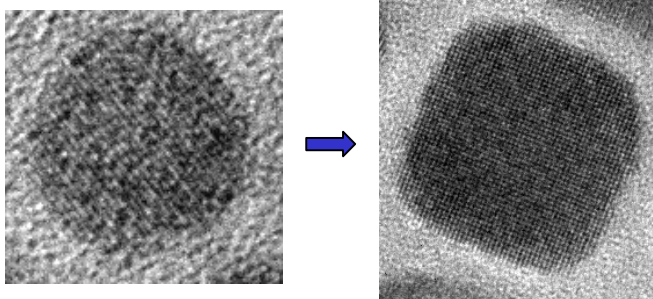
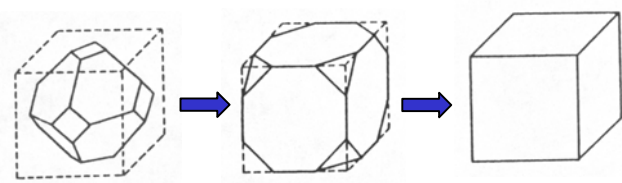


WAXS of 10 nm PbSe quantum cubes slowly deposited from toluene (top) and rapidly precipitated from methanol (bottom)

Shape evolution of PbSe Nanocrystals



Highly symmetric rock salt structure



Modeling of x-ray diffraction:

The Debye equation which is valid in the kinematical approximation is shown in equation 4.6⁽⁸⁾.

$$I(q) = I_0 \sum_m \sum_n F_m F_n \frac{\sin(qr_{m,n})}{qr_{m,n}}$$

(4.6)

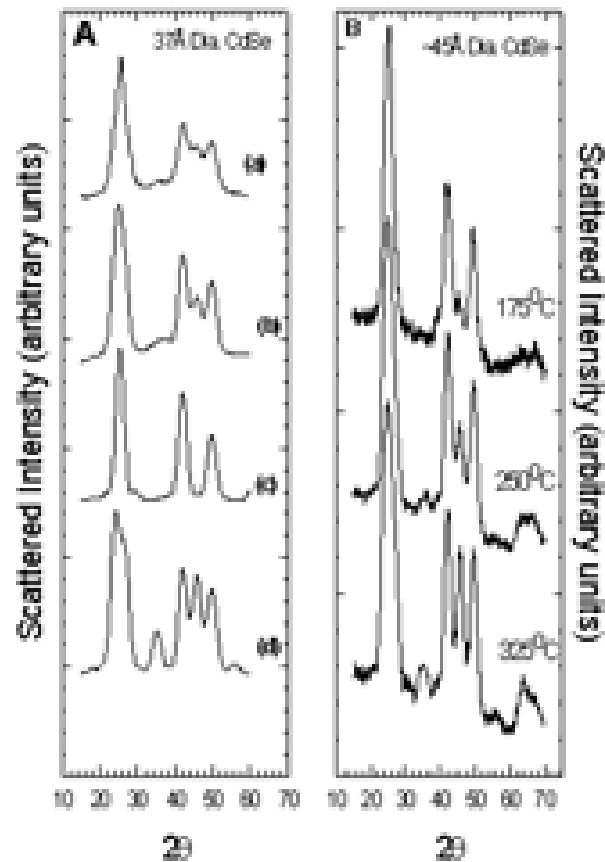
Where $I(q)$ is the scattered intensity , I_0 is the incident intensity, q is the scattering parameter [$q = 4\pi\sin(\theta)/\lambda$] for X-rays of wavelength λ diffracted through angle θ .

The distance between atoms m and n is r_{mn} . A discrete form of the Debye is shown in equation (4.7)⁽⁹⁾.

(4.7)

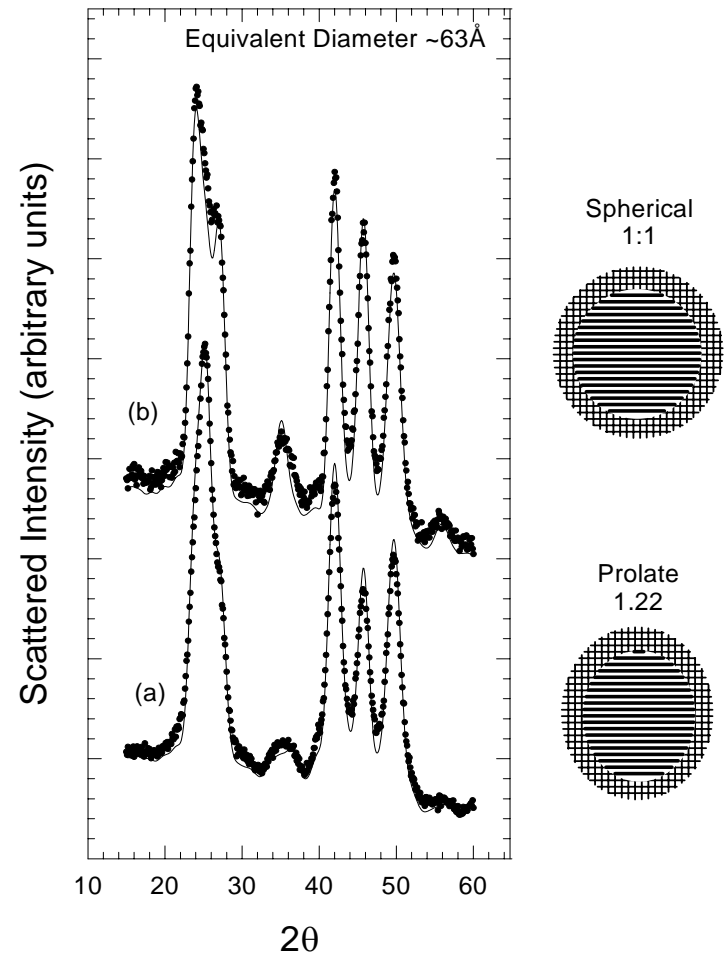
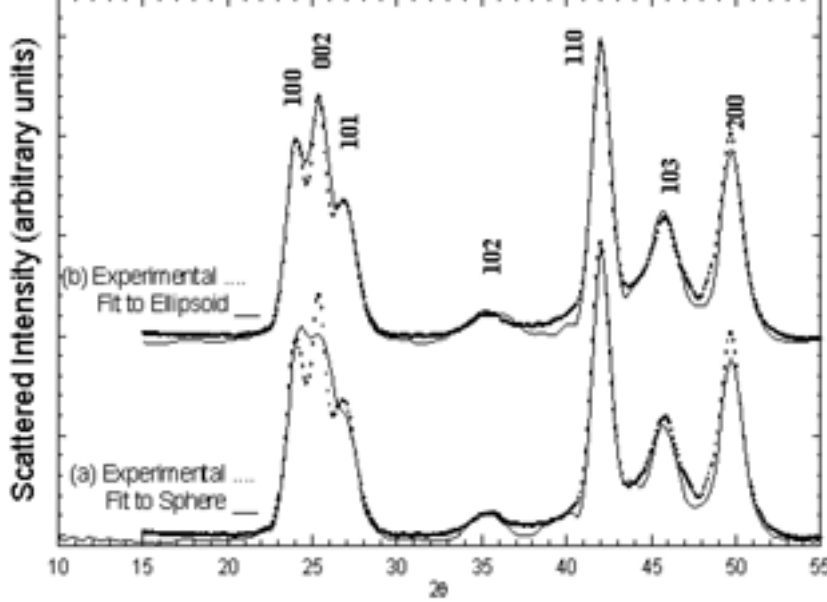
$$I(q) = I_0 \frac{f^2(q)}{q} \sum_k \frac{\rho(r_k)}{r_k} \sin(qr_k)$$

where I_0 is the incident intensity, $f(q)$ is the angle dependent scattering factor q is the scattering parameter [$4\pi\sin(\theta)/\lambda$] for X-rays of wavelength λ diffracted through angle θ . The sum is over all inter atomic distances, and $\rho(r_k)$ is the number of times a given interatomic distance r_k occurs. Since the number of discrete interatomic distances in an ordered structure grows much more slowly than the total number of distances, using the discrete form of the equation is significantly more efficient in the simulation of large crystallites⁽⁹⁾.



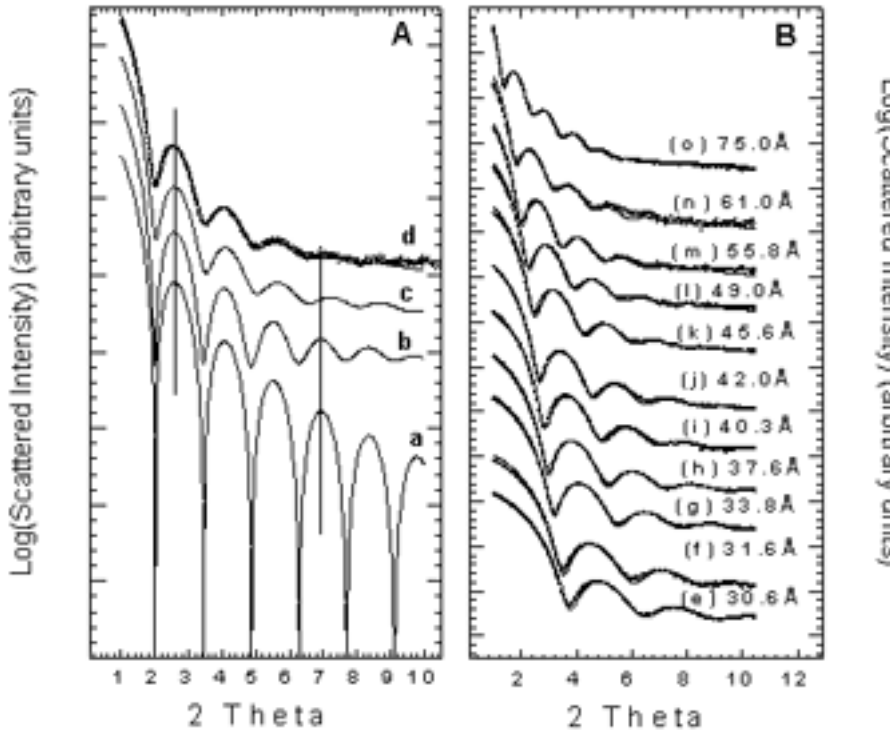
Modeling NP Shape

Modeling Stacking faults



20

Small angle X-ray Scattering SAXS



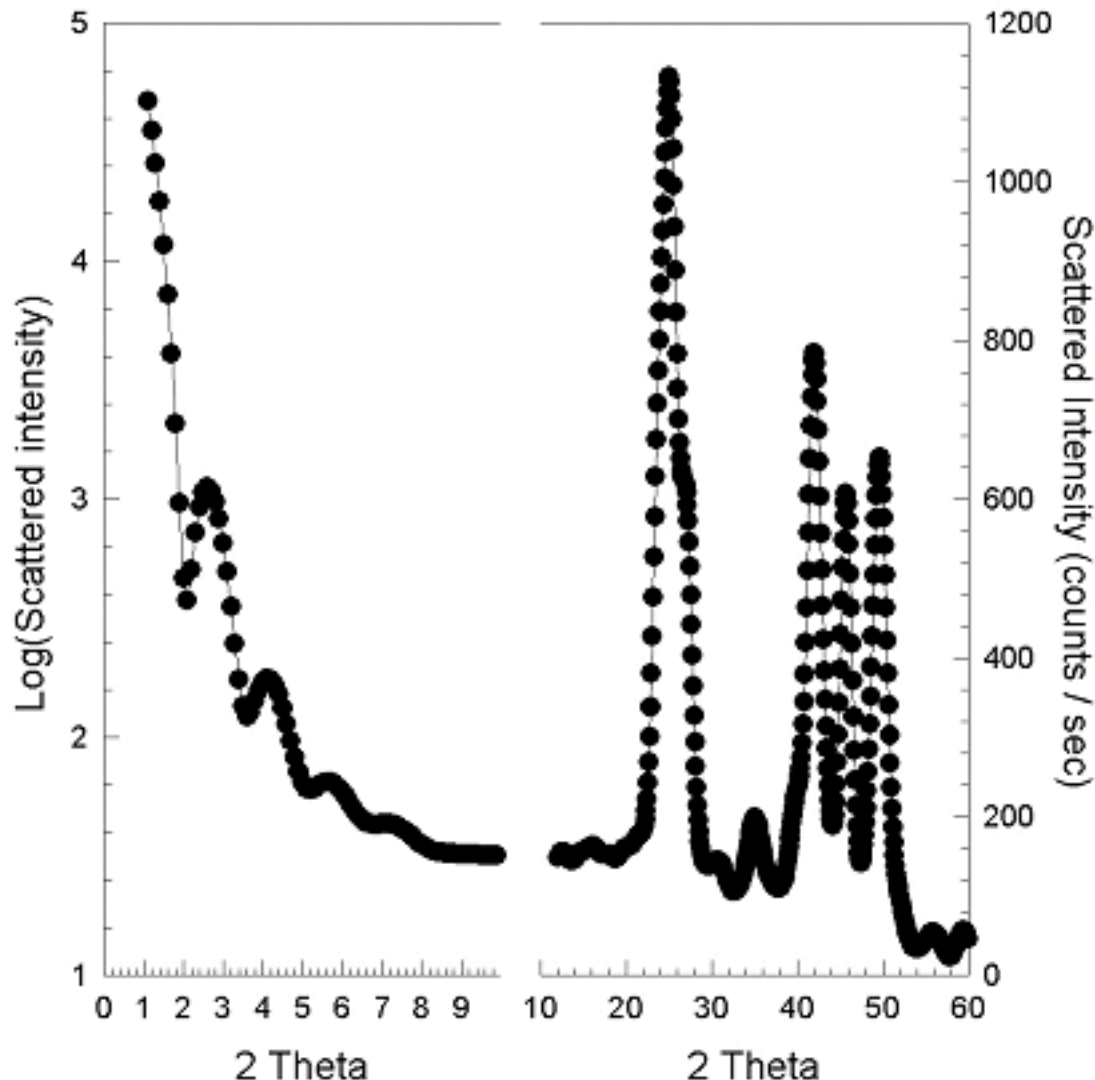
$$(4.8) \quad I(q) = I_o N [(\rho - \rho_o)^2 \frac{4}{3} \pi R^3 [3 \frac{\sin(qR) - qR \cos(qR)}{(qR)^3}]]^2$$

Where ρ and ρ_o are the electron density of the particle and the dispersing medium respectively. I_o is the incident intensity and N is the number of particles. $F(q)$ is the material form factor (the fourier transform of the shape of the scattering object) and is the origin of the oscillations observed. Thus for a spherical particle of radius R

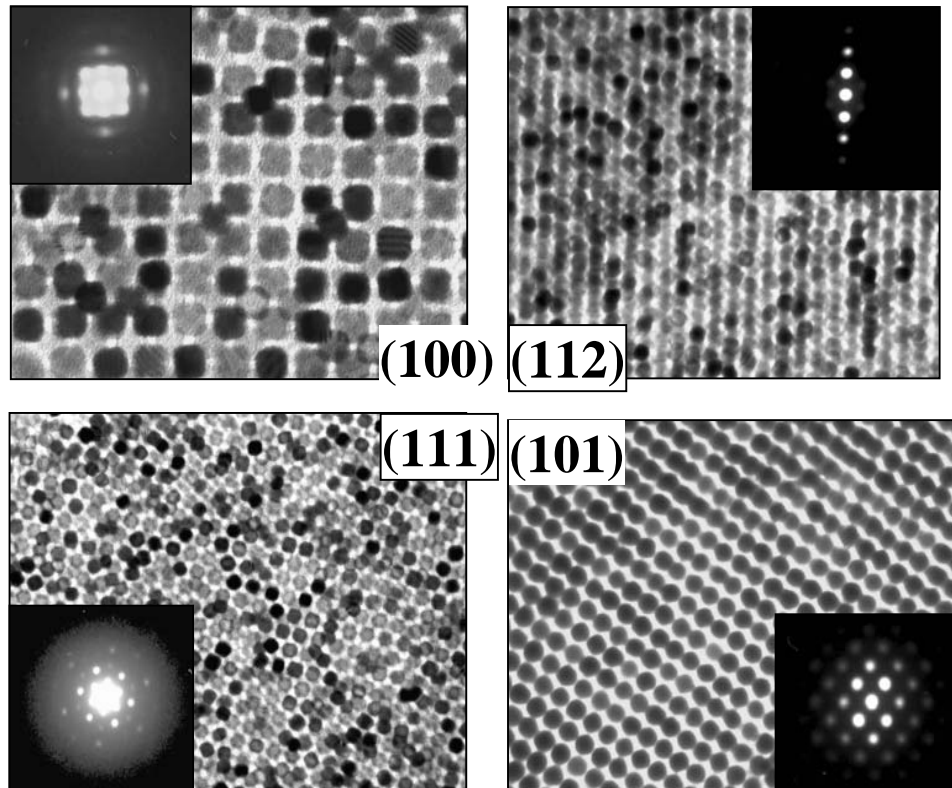
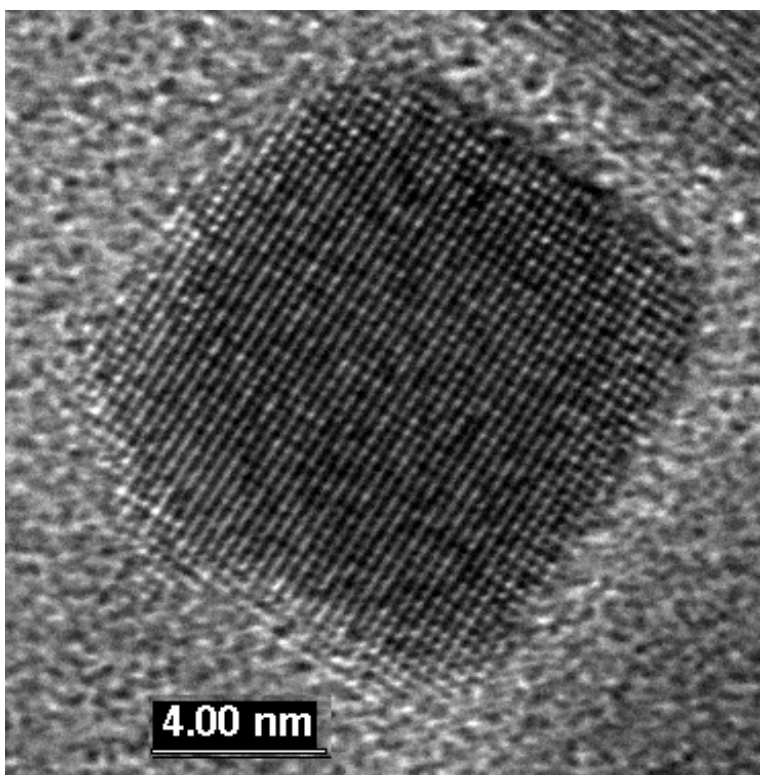
$$(4.9) \quad I(q) = I_o N (\rho - \rho_o)^2 F^2(q)$$

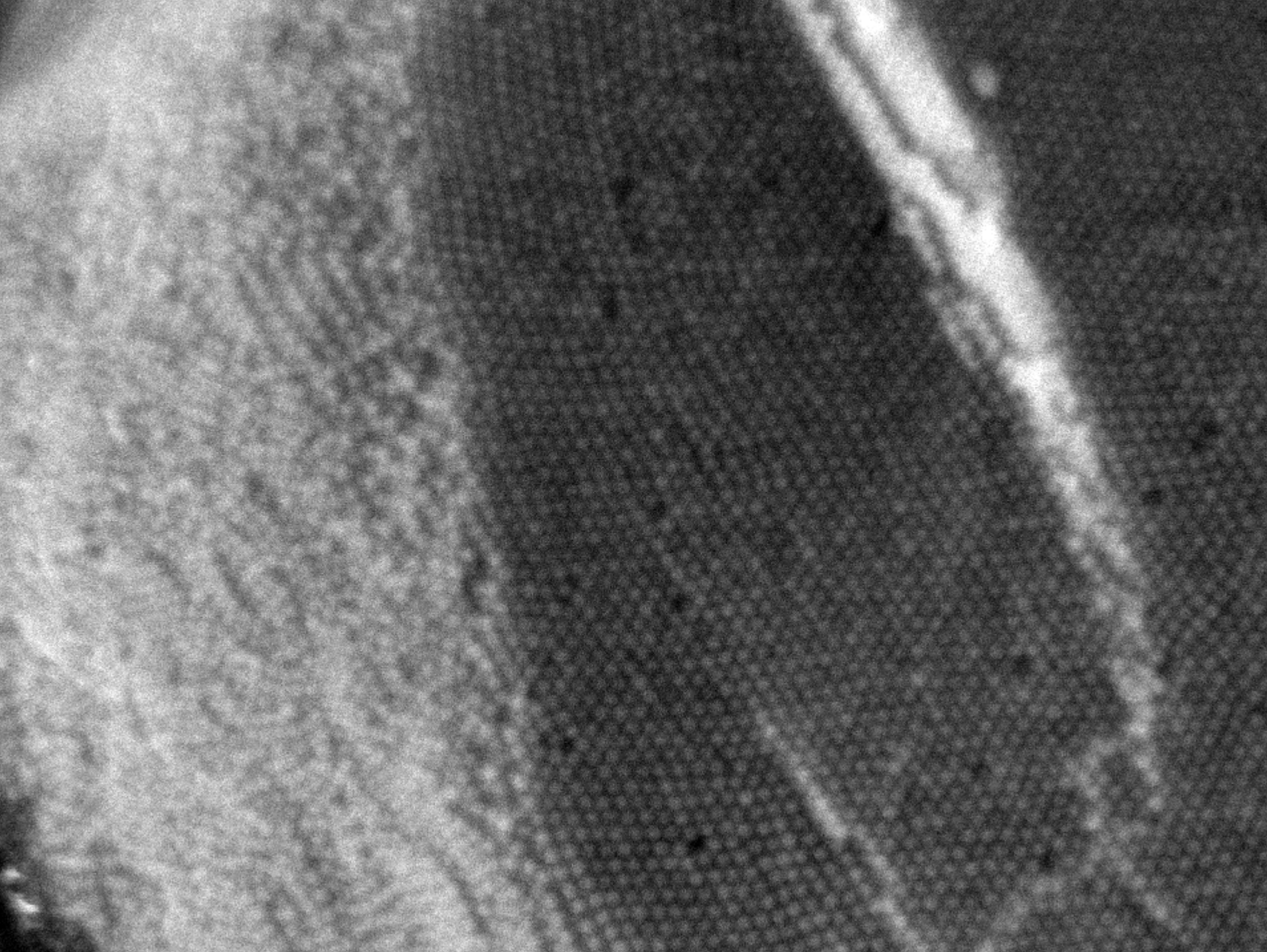
$$(4.10) \quad F(q) = \frac{4}{3} \pi R^3 [3 \frac{\sin(qR) - qR \cos(qR)}{(qR)^3}]$$

Combined SAXS and WAXS Modeling.

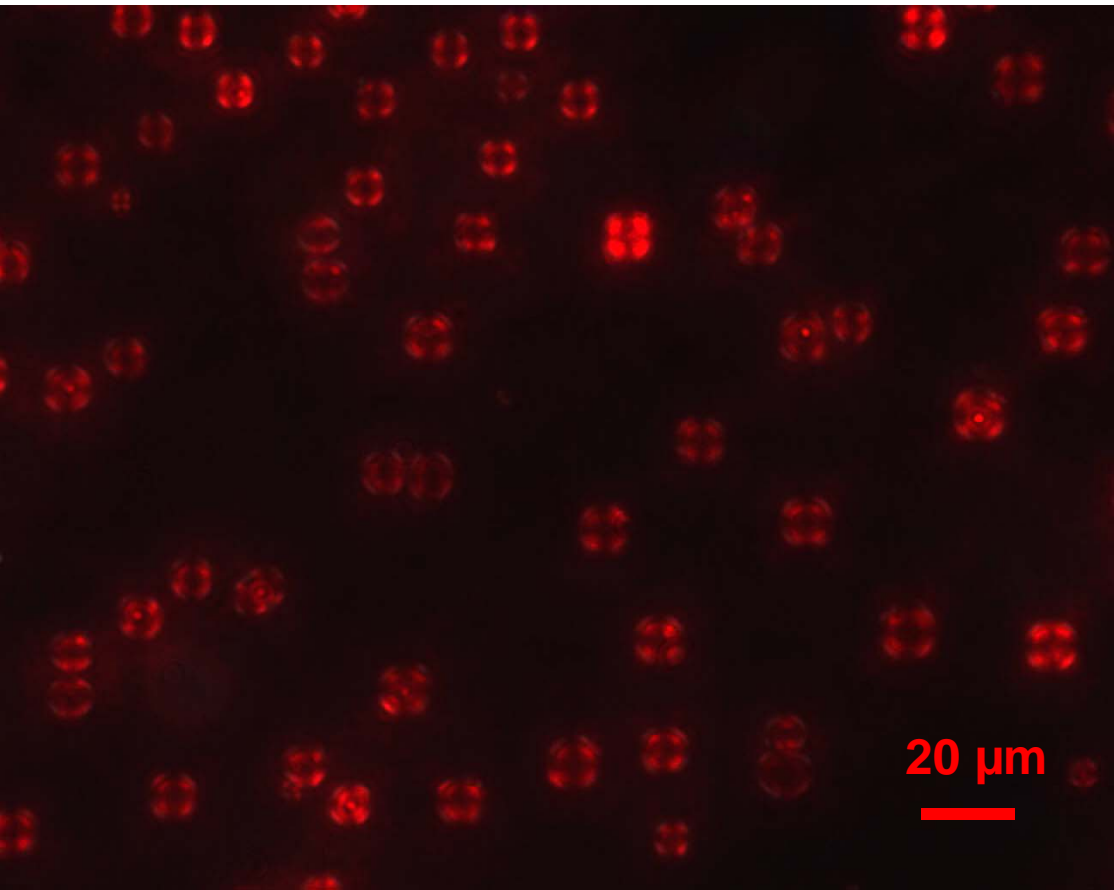


Qunatum cubes: Cubic 12 nm PbSe nanocrystals Assembling into a superlattice.



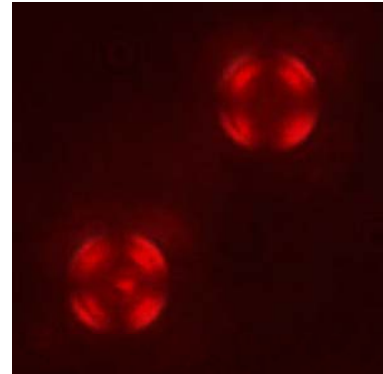


Self-assembled CdSe nanorod solids



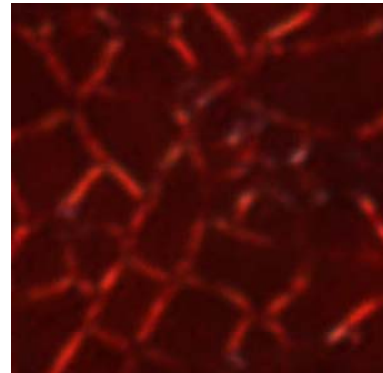
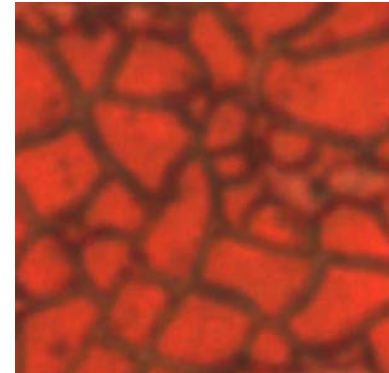
*without
polarizers*

*with
crossed
polarizers*

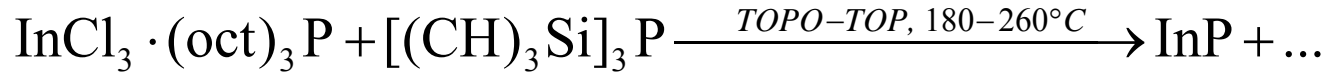


20 μm

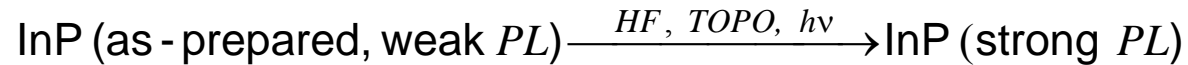
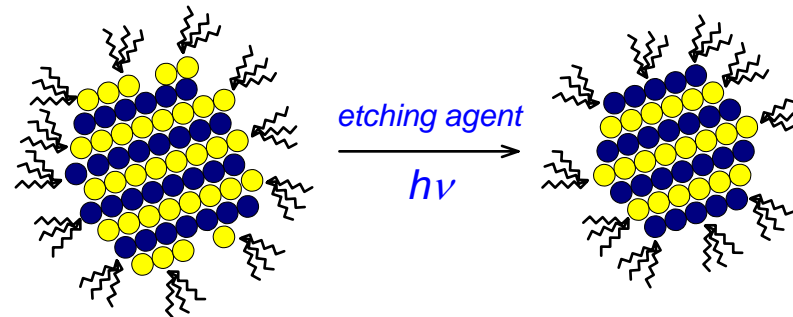
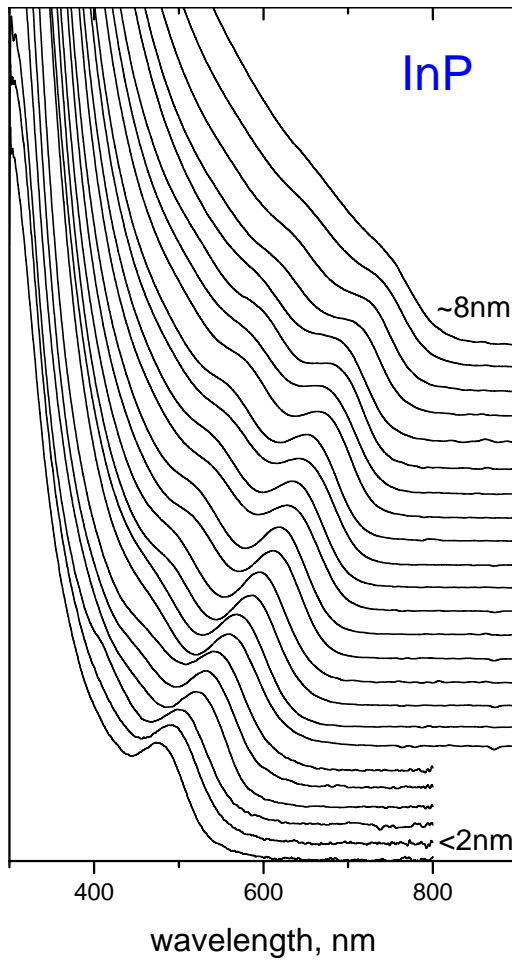
*Optical micrograph of self-assembled CdSe
nanorods (between crossed polarizers).*



III-V semiconductor nanocrystals : InP



absorbance, a.u.



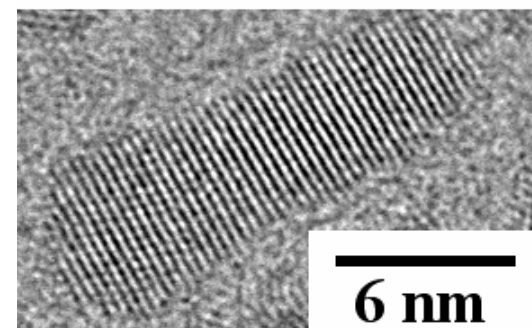
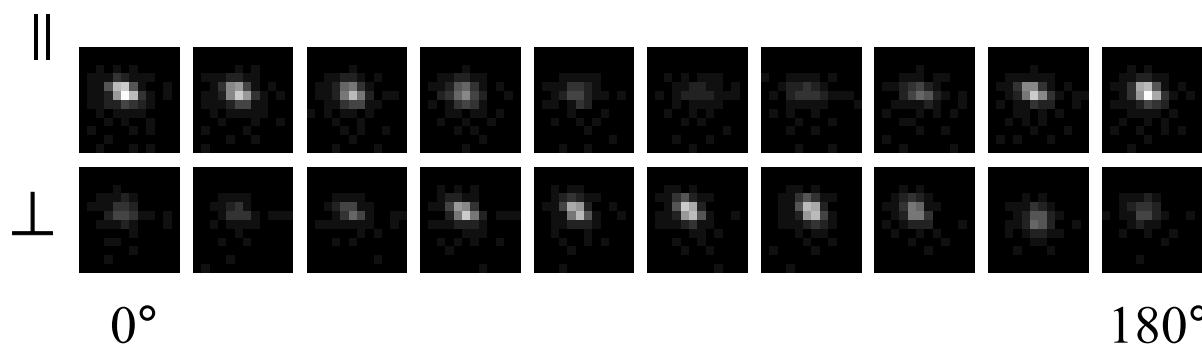
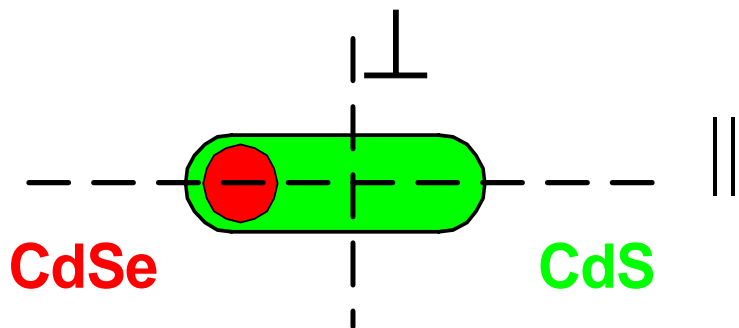
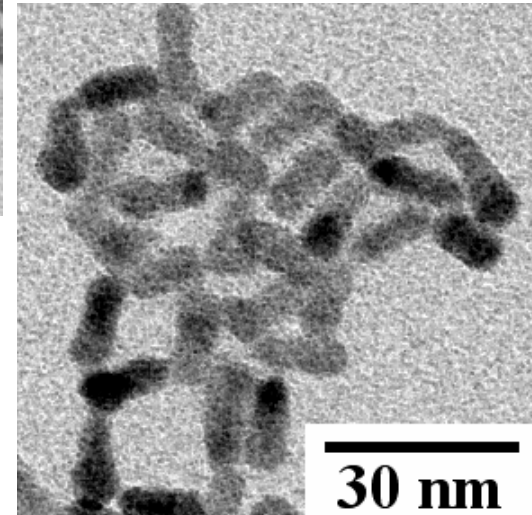
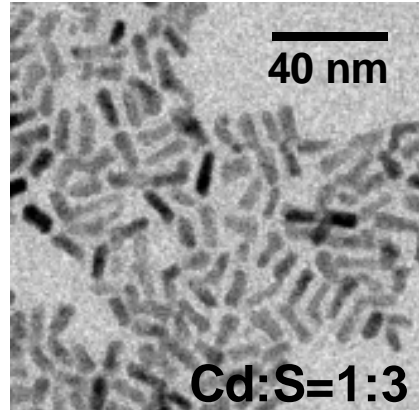
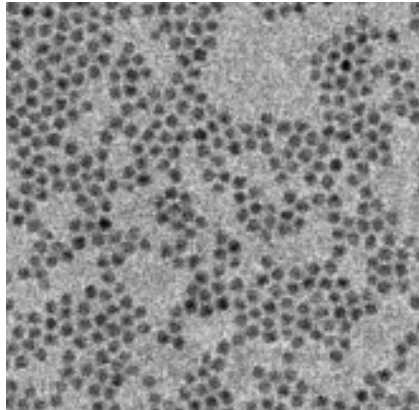
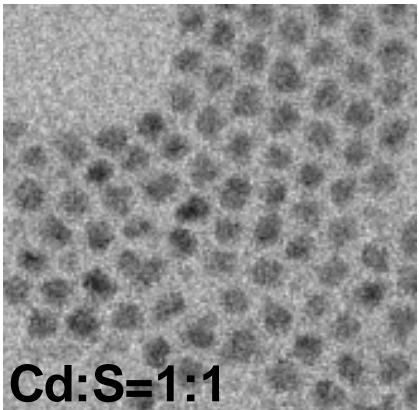
PL quantum efficiency ~25-40%

Size-dependent evolution of absorption spectra of InP colloidal quantum dots

J. Phys. Chem. B, 2002, 106, 12659.

CdSe/CdS quantum dot - quantum rods

CdSe/CdS ← CdSe cores → CdSe/CdS

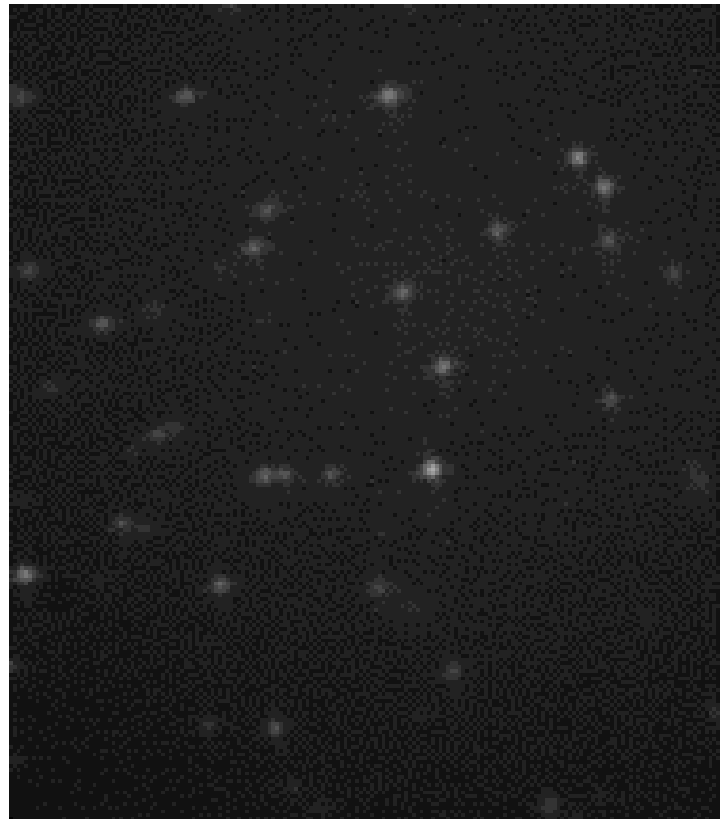


Luminescent II-VI nanocrystals

Room temperature PL quantum efficiencies 50-70%

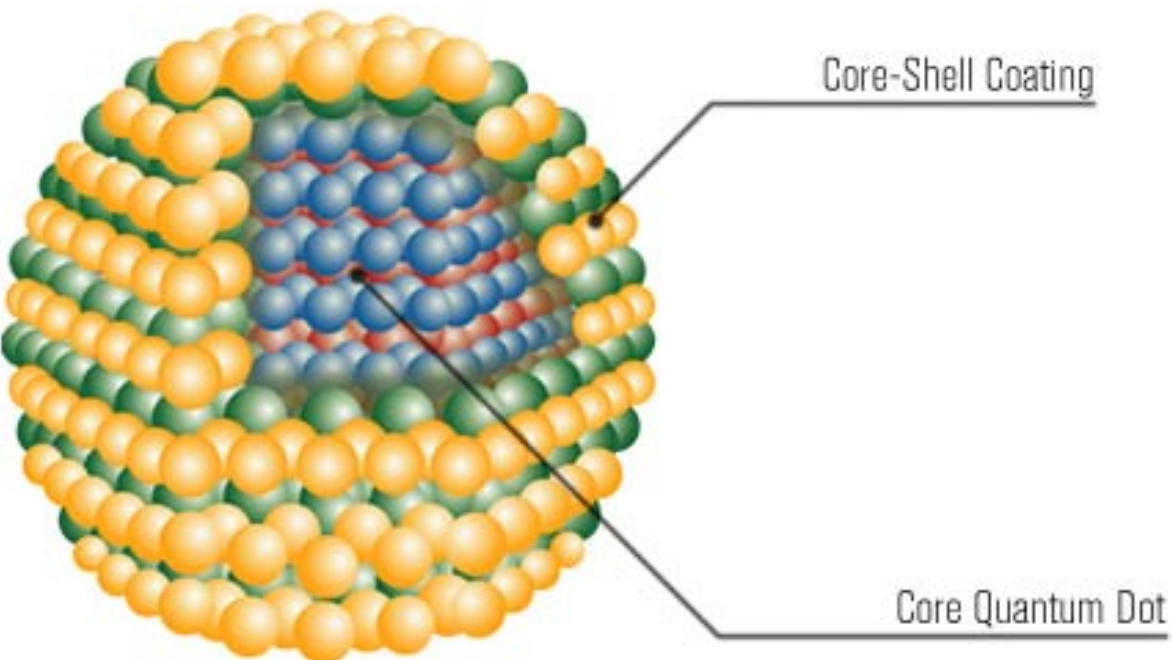


Colloidal solutions of CdSe/ZnS core-shell nanocrystals.



Single particle luminescence of CdSe/ZnS nanocrystals

CdSe/CdS core-shell nanocrystals in a polymer matrix



CORE-SHELL EviDOT

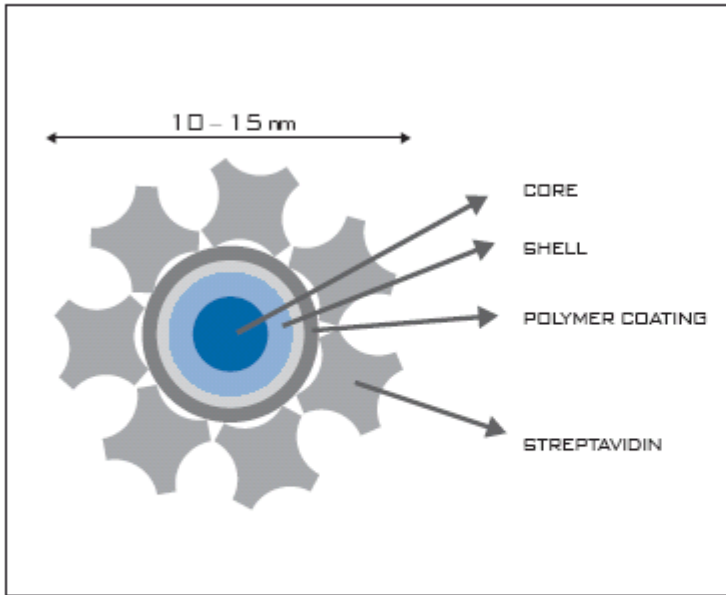


FIGURE 1. DIAGRAM OF A QDOT STREPTAVIDIN CONJUGATE. The layers represent the distinct structural elements of the Qdot nanocrystal and are roughly to scale. As shown Qdot quantum dots contain a semiconductor (CdSe) nanocrystal core, a semiconductor (ZnS) shell, then a polymer coat, and finally streptavidin on the outer surface.

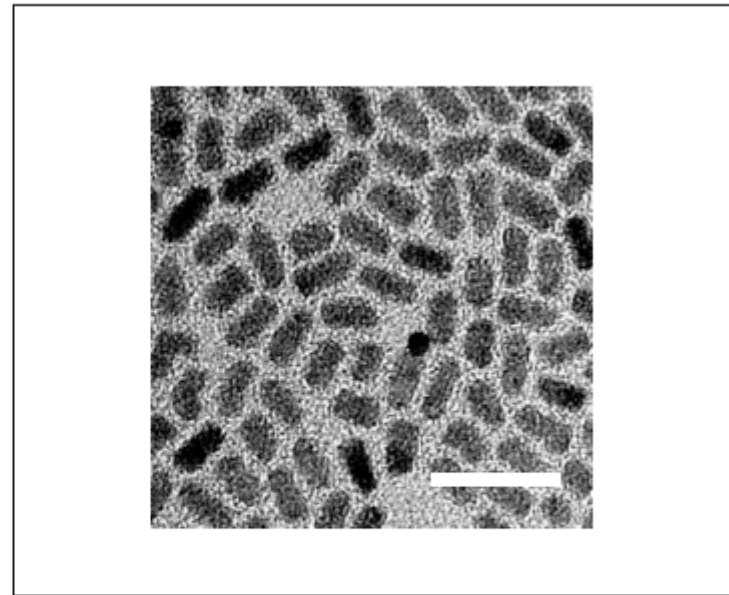


FIGURE 2. TRANSMISSION ELECTRON MICROGRAPH OF QDOT CORE-SHELL NANOPARTICLES. Shown at 200,000X magnification. Scale bar = 20 nm.

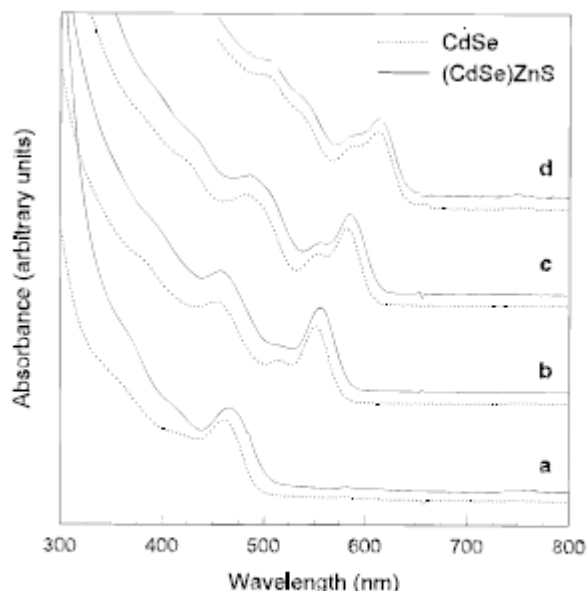


Figure 1. Absorption spectra for bare (dashed lines) and 1–2 monolayer ZnS overcoated (solid lines) CdSe dots with diameters measuring (a) 23, (b) 42, (c) 48, and (d) 55 Å. The absorption spectra for the (CdSe)ZnS dots are broader and slightly red-shifted from their respective bare dot spectra.

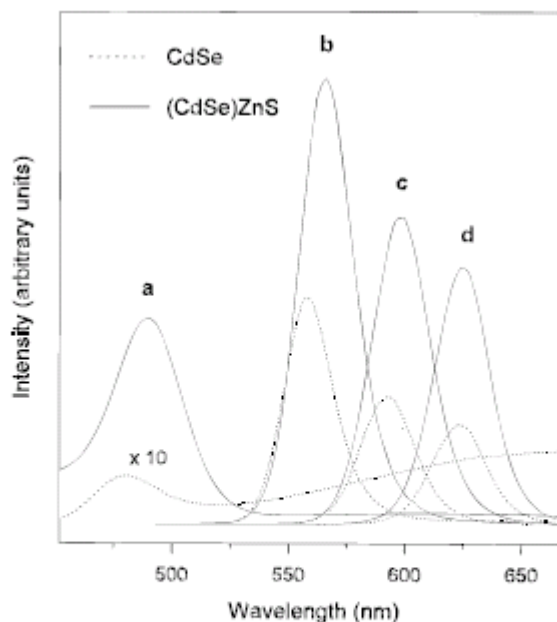


Figure 2. Photoluminescence (PL) spectra for bare (dashed lines) and ZnS overcoated (solid lines) dots with the following core sizes: (a) 23, (b) 42, (c) 48, and (d) 55 Å in diameter. The PL spectra for the overcoated dots are much more intense owing to their higher quantum yields: (a) 40, (b) 50, (c) 35, and (d) 30.

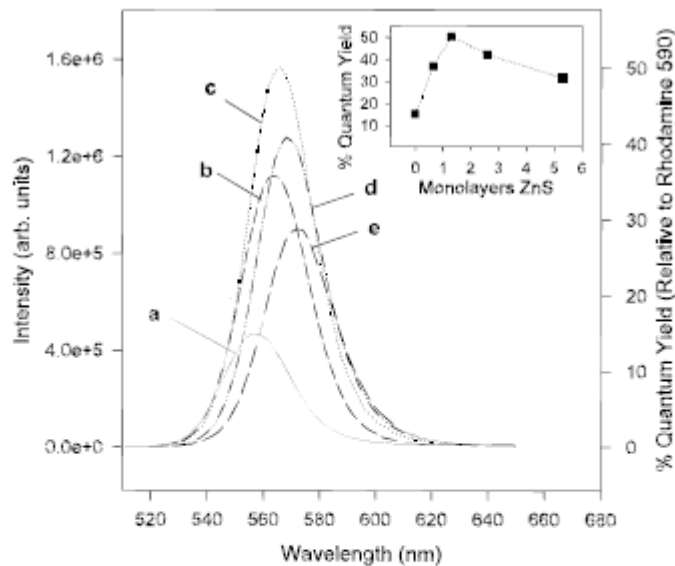


Figure 5. PL spectra for a series of ZnS overcoated dots with $42 \pm 10\text{ \AA}$ diameter CdSe cores. The spectra are for (a) 0, (b) 0.65, (c) 1.3, (d) 2.6, and (e) 5.3 monolayers ZnS coverage. The position of the maximum in the PL spectrum shifts to the red, and the spectrum broadens with increasing ZnS coverage. (inset) The PL quantum yield is charted as a function of ZnS coverage. The PL intensity increases with the addition of ZnS reaching, 50% at ~ 1.3 monolayers, and then declines steadily at higher coverage. The line is simply a guide to the eye.

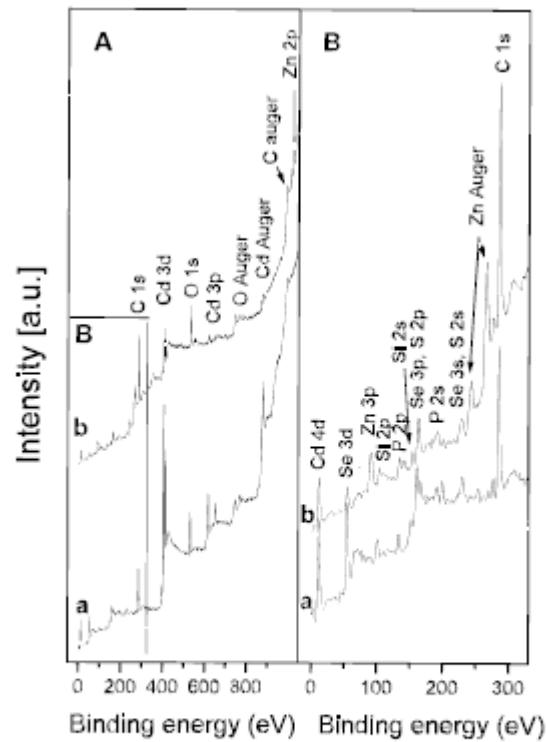


Figure 6. (A) Survey spectra of (a) $\sim 40\text{ \AA}$ diameter bare CdSe dots and (b) the same dots overcoated with ZnS showing the photoelectron and Auger transitions from the different elements present in the quantum dots. (B) Enlargement of the low-energy side of the survey spectra, emphasizing the transitions with low binding energy.

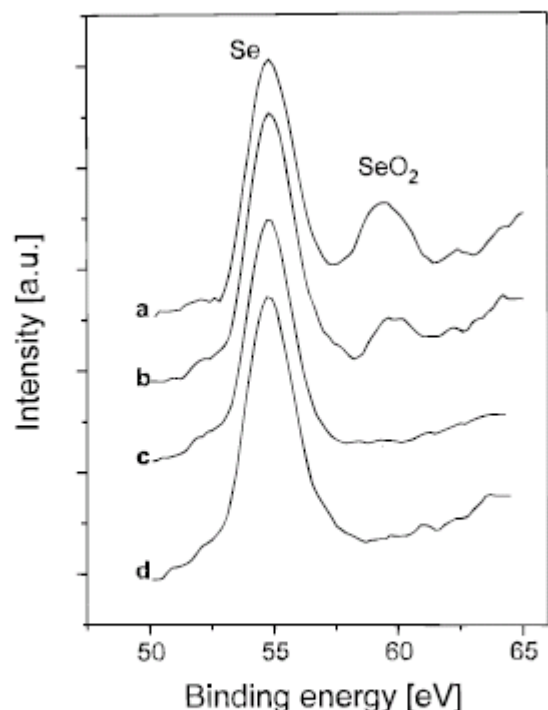


Figure 7. X-ray photoelectron spectra highlighting the Se 3d core transitions from $\sim 40 \text{ \AA}$ bare and ZnS overcoated CdSe dots: (a) bare CdSe, (b) 0.65 monolayers, (c) 1.3 monolayers, and (d) 2.6 monolayers of ZnS. The peak at 59 eV indicates the formation of selenium oxide upon exposure to air when surface selenium atoms are exposed.

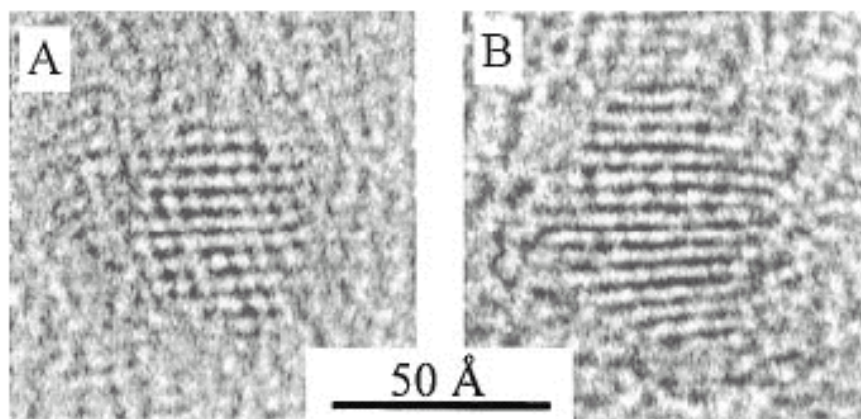


Figure 8. Transmission electron micrographs of (A) one “bare” CdSe nanocrystallite and (B) one CdSe nanocrystallite with a 2.6 monolayer ZnS shell.